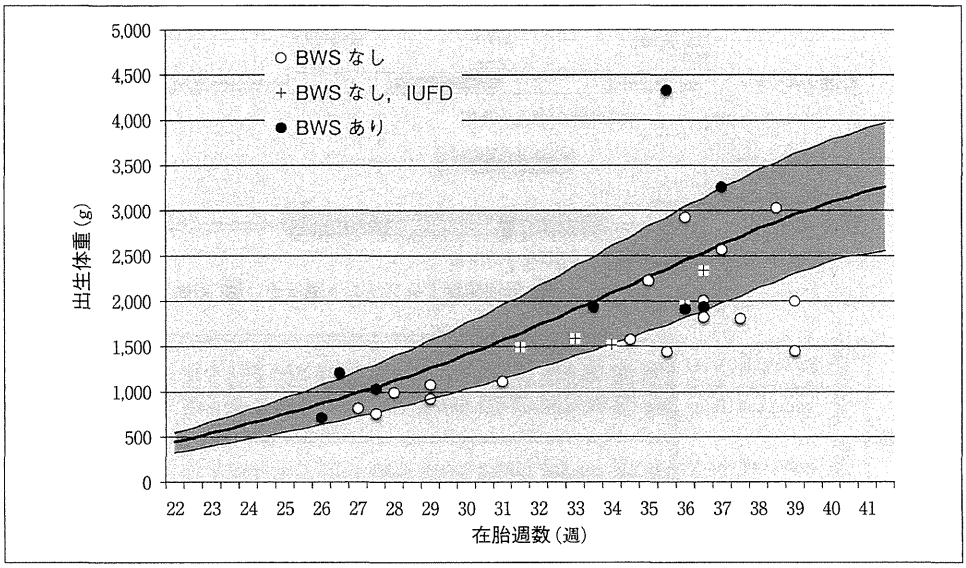

図2　PMD国内症例の在胎週数と出生体重　これまでに我々が集積した本邦のPMD症例のうち，分娩に至った31症例について在胎週数（週）と出生体重（g）の関連を示す．比較のために日本人の胎児発育曲線（m, m±2.0SD）を実線で例示した．週数に比して大きい児（HFD児）は3例で，全てBWSを合併した児であった．週数に比して小さい児（LFD児）は8例であった．出生体重が4,000 gを超える巨大児は1例のみであった．

IUFDは妊娠31～36週に生じており，興味深いことに全てBWSを合併していない症例であった．IUFDの発生率は，1975～2005年における海外症例の35.6%より低率であった．5例中2例が胎児発育不全fetal growth restriction（FGR）を指摘されていたが，出生に至った児と比較しても特にFGRの傾向が強いわけではなかった．IUFDの予知因子を解明することも今後の課題だが，今回集積した症例では，妊娠25週以降に産科的適応でターミネーションが施行された結果，児が救命されていることが多かった．本邦の高リスク妊娠に対する周産期医療提供体制は，PMDにおける児の生存率改善にも有効であると推定される．

表2　間葉性異形成胎盤（PMD）の特徴（文献8より抜粋）

1. 1個の胎盤としての形態を備えている．
2. 肉眼的に部分胞状奇胎に類似する．
3. 血管の走行は蛇行し異形成の外観を呈する．
4. 水腫様変化の絨毛には血管がある．栄養膜細胞の異常増殖はない．
5. 絨毛血管内に間葉系の細胞の増生があり，血管内には多発性の血栓がみられる．
6. 胎児はsmall for dates（子宮内胎児発育遅延）であることが多いが，BWS症例を除き奇形はない．

Ⅱ．PMDの原因遺伝子

1．インプリント遺伝子

インプリント遺伝子とは，一対の対立遺伝子のうち一方の親由来遺伝子のみが発現する（片アレル発現）遺伝子のことで，個体の発生・発育・成長，胎盤形成などに重要な役割を担っている．約25%のPMDにインプリンティング疾患であるBWSを合併することから，BWSの責任領域である11p15領域のインプリント異常の関連が示唆されてきた．11p15には複数のインプリント遺伝子が存在するが，BWSの症状に関連する遺伝子は*IGF2*と*CDKN1C*（$p57^{KIP2}$，*KIP2*）である（**図3a**）．*IGF2*は，細胞増殖を促進するインスリン様増殖因子をコードしており，父性アレルからのみ発現する（父性片アレル発現）．また，*IGF2*は胎盤の成長に重要である．一方，*CDKN1C*は，細胞増殖を抑制するサイクリン依存性キナーゼ阻害因子をコードしており，母性片アレル発現を示す．$p57^{KIP2}$はPMD胎盤の細胞性栄養膜細胞にのみ発現し，絨毛内の間質や血管では発現していないこと[9]，BWSのモデルマウス（$p57^{KIP2}$母性アレル欠失と*IGF2*の両アレル発現（loss of imprinting）を同時にもつ）の胎盤は腫大しPMDに類似した異形成像を示すことから[10]，*IGF2*と$p57^{KIP2}$はPMDの原因遺伝子の候補と考えられている．

PMDは2倍体で，大半は46,XXの核型を示す．2006年頃よりPMDの発症にandrogenetic/biparentalモザイクあるいはキメラが関与する可能性が報告された[11]．androgenetic細胞だけの場合は全胞状奇胎となるが，PMDはbiparental細胞（父由来ゲノムと母由来ゲノムを1セットずつもつ正常細胞）とのモザイクあるいはキメラであり，胎児が存在する．androgenetic細胞の46本の染色体は全て父由来なので，当然なが

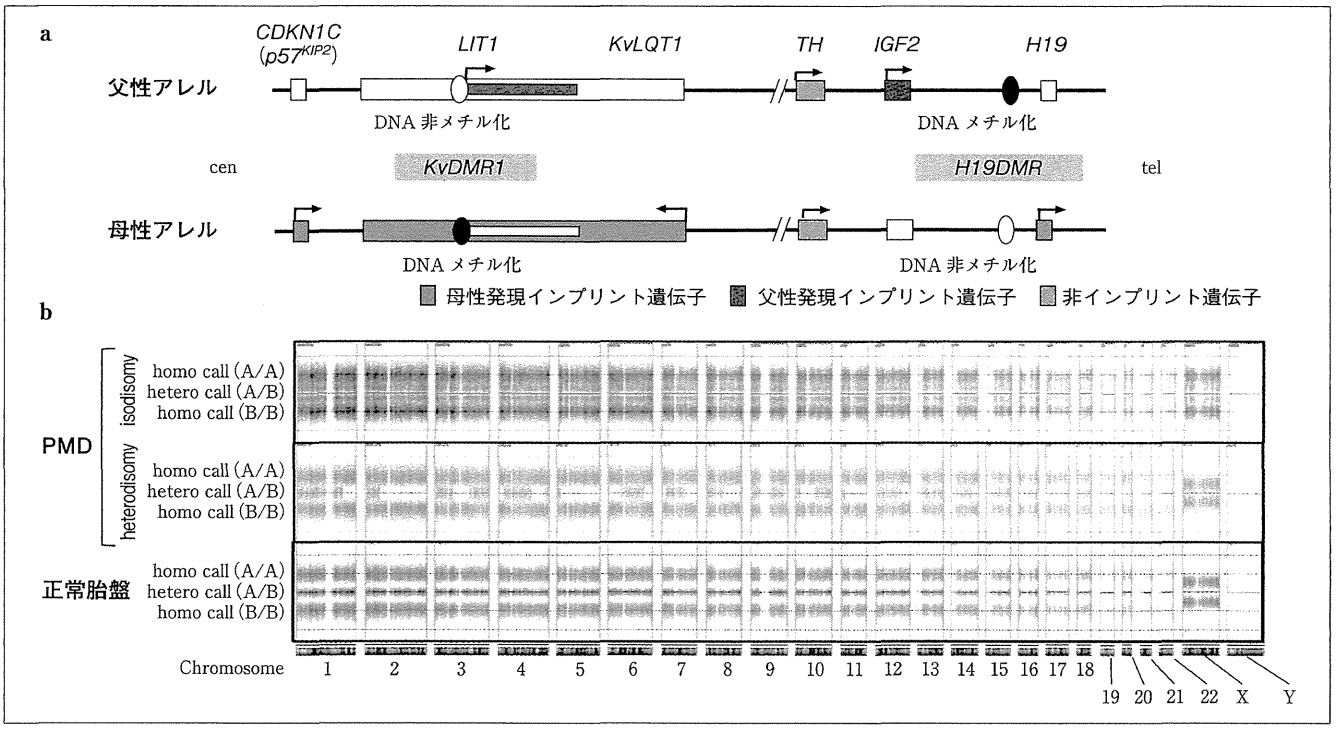

図3　11p15のインプリンティング領域とPMD胎盤のSNPアレイ解析　a：11p15のインプリンティング領域．本領域には，複数のインプリント遺伝子が存在する(代表的な遺伝子のみ記す)．KvDMR1とH19DMRは，アレル間でDNAメチル化が異なる領域(DNA可変領域：DMR)である．KvDMR1は*CDKN1C*と*LIT1*の発現を調節し，H19DMRは*IGF2*と*H19*の発現を調節する．androgenetic/biparentalモザイクのandrogenetic細胞では，父性アレルが2コピーで母性アレルがゼロコピーとなるため，$p57^{KIP2}$の発現減少と*IGF2*の発現増加が生じる．cen：セントロメア側，tel：テロメア側．b：SNPアレイ解析．PMD胎盤よりDNAを抽出し，Genome-Wide Human SNP array 6.0(Affymetrix)で解析した．正常受精卵における母性ゲノムの複製不全でandrogenetic/biparentalモザイクが生じた場合は，isodisomyとなる．正常胎盤に比べhetero call (A/B)を示すシグナルが消失し，homo call(A/A，B/B)を示すシグナルが縦に幅広く検出される．本症例のモザイク率が低いため，homo callが幅広くなっている．一方，二精子受精によるandrogenetic/biparentalモザイクあるいは2つの受精卵によるandrogenetic/biparentalキメラの場合は，heterodisomyとなる．heterodisomyの場合は，2つの精子のハプロタイプの違いを反映して，hetero callが消失しhomo callのみが検出される領域とhetero callとhomo callを検出する領域が混在する．

ら11p15領域も父性アレルが2コピー存在する(母性アレルはゼロコピー)．そのため，*IGF2*の発現増加と$p57^{KIP2}$の発現減少が生じ，PMD発生につながると考えられる．androgenetic細胞は，絨毛膜の胚外中胚葉extra-embryonic mesoderm，脈管に分布し，trophoblastには存在しない[11]．胞状奇胎と異なりtrophoblastの異常増殖を認めないのはこのためと考えられる．androgenetic/biparentalモザイク・キメラはPMDの大半の症例で認められ，自験例でもSNP(single nucleotide polymorphism)アレイ解析により検出している(**図3b**)．しかし，ゲノム中には100個程度のインプリント遺伝子が存在するため，*IGF2*と$p57^{KIP2}$以外のインプリント遺伝子の発現異常も生じていると考えられる．また，androgenetic/biparentalモザイク・キメラを認めないPMD症例も存在することからも，他のインプリント遺伝子(あるいは非インプリント遺伝子)が関与している可能性がある．

androgenetic/biparentalモザイク・キメラの発生機序については，以下の3つが考えられている[12](**図4**)．①正常受精における母性ゲノムの複製不全：23,X精子が卵と受精した後，母性ゲノムが複製せず，父性ゲノムのみが複製し細胞分裂が生じる．複製しなかった母性ゲノムと父性ゲノムをもつ娘細胞は46,XXのbiparental細胞となる．他方の娘細胞は父性ゲノム(23,X)の1倍体となるが，核内倍加が起こりandrogenetic細胞となる．これにより，androgenetic(46,XX)/biparental(46,XX)モザイクが生じる．androgenetic細胞は1精子由来のゲノムの2倍体であるため，isodisomyである(**図4a**)．23,Y精子が受精した場合は，46,YY細胞が生存できないため，

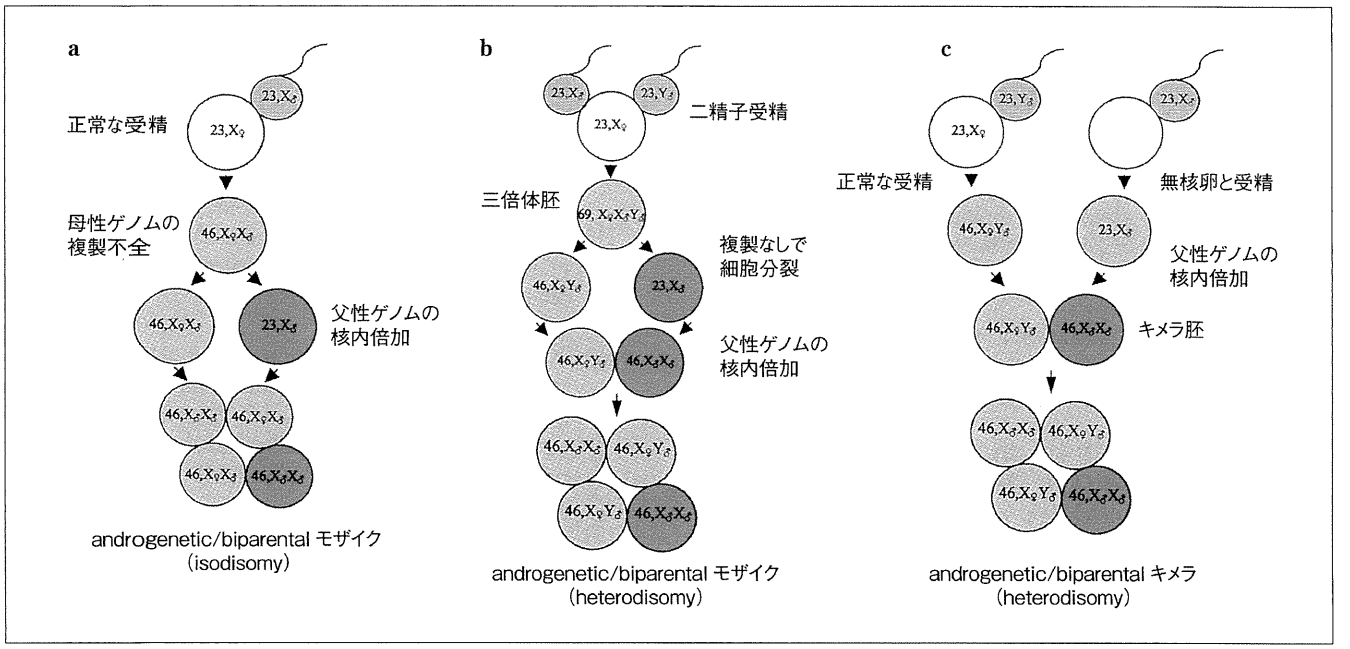

図4　androgenetic/biparental モザイク・キメラの発生機序　a：正常受精における母性ゲノムの複製不全．b：二精子受精．c：2つの受精卵によるキメラ．詳細は本文参照．（文献12より改変）

androgenetic/biparentalモザイクにはならない．②二精子受精：2つの精子(23,Xと23,Y)が卵と受精し3倍体の受精卵となったあと，複製なしに細胞分裂が生じ，46,XYのbiparental細胞と23,X(精子由来)の1倍体細胞が生じる．1倍体細胞で核内倍加が起こりandrogenetic細胞となるため，androgenetic(46,XX)/biparental(46,XY)モザイクが生じる．父性ゲノムは2つの精子に由来するためheterodisomyとなる(**図4b**)．③2つの受精卵によるキメラ：無核卵に23,X精子が受精し，核内倍加が起こりandrogenetic細胞となる．一方で，正常受精卵(46,XY)も同時に生じた場合，2つの受精卵からキメラが形成されるため，androgenetic(46,XX)/biparental(46,XY)キメラとなる．この場合も，父性ゲノムは2つの精子に由来するためheterodisomyとなる(**図4c**)．②と③を識別することは困難である．実際は①によるandrogenetic/biparentalモザイクが大半を占める．

2. VEGF-D - VEGFR-3シグナル伝達系

PMDは女児に多く，幹絨毛血管に異常を認めることから[13]，X染色体上(Xp22.31)にマップされるvascular endothelial growth factor D (VEGF-D)が候補遺伝子として考えられている．1例ではあるが，PMD胎盤の嚢胞でVEGF-Dの発現が亢進している報告がある[14]．また，VEGF-Dの受容体であるVEGFR-3が胎盤嚢胞や末端絨毛血管の内皮で発現していることも報告されていることから[14,15]，VEGF-D - VEGFR-3シグナル伝達系がPMD発生に関与している可能性が示唆されている．

おわりに

PMDは新しい疾患概念で，頻度が極めて低いことから，病態の認知度が低かった．しかし，2007年以降，論文数・症例報告数が急増していることから，国内外での認知が進んでいることが窺える．今後，未知の原遺伝子を同定し，病態の理解が深まることが期待される．また，散発的な研究ではなく，大規模な前向き調査を行うことで，遺伝子診断も含めた診断基準確立や診療ガイドラインを策定することが肝要と思われる．

謝辞：PMDの肉眼所見をご提供いただいた北海道大学産科・周産母子センター 山田崇弘博士に深謝申し上げます．本稿で紹介した研究結果は，厚生労働科学研究費補助金難治性疾患等克服研究事業「間葉性異形成胎盤の臨床的・分子遺伝学的診断法の開発を目指した基盤研究」によりサポートされたものです．

文　献

1) Moscoso, G., Jauniaux, E., Hustin, J.：Placental vascular anomaly with diffuse mesenchymal stem villous hyperplasia. A new clinico-pathological entity? Pathol Res Pract 1991, **187**：324-328
2) Lage, J.M.：Placentomegaly with massive hydrops of placental stem villi, diploid DNA content, and fetal omphaloceles：possible association with Beckwith-Wiedemann syndrome. Hum Pathol 1991, **22**：591-597
3) Sebire, N.J.：Gestational trophoblastic neoplasia. Ultrasonography in Obstetrics and Gynecology (Callen, P.W. ed.), Elsevier, Philadelphia, 2008, 951-967
4) Chen, C.P., Chern, S.R., Wang, T.Y. et al.：Pregnancy with concomitant chorangioma and placental vascular malformation with mesenchymal hyperplasia. Hum Reprod 1997, **12**：2553-2556
5) Cohen, M.C., Roper, E.C., Sebire, N.J. et al.：Placental mesenchymal dysplasia associated with fetal aneuploidy. Prenat Diagn 2005, **25**：187-192
6) Manipalviratn, S., DeCherney, A., Segars, J.：Imprinting disorders and assisted reproductive technology. Fertil Steril 2009, **91**：305-315
7) 緒方　勤，鏡　雅代：生殖補助医療とインプリンティング異常症. J Mamm Ova Res 2006, **23**：158-162
8) 中山雅弘：目で見る胎盤病理，医学書院，東京，2002
9) Allias, F., Lebreton, F., Collardeau-Frachon, S. et al.：Immunohistochemical expression of p57 in placental vascular proliferative disorders of preterm and term placentas. Fetal Pediatr Pathol 2009, **28**：9-23
10) Caspary, T., Cleary, M.A., Perlman, E.J. et al.：Oppositely imprinted genes *p57^{Kip2}* and *Igf2* interact in a mouse model for Beckwith-Wiedemann syndrome. Genes Dev 1999, **13**：3115-3124
11) Kaiser-Rogers, K.A., McFadden, D.E., Livasy, C.A. et al.：Androgenetic/biparental mosaicism causes placental mesenchymal dysplasia. J Med Genet 2006, **43**：187-192
12) Morales, C., Soler, A., Badenas, C. et al.：Reproductive consequences of genome-wide paternal uniparental disomy mosaicism：description of two cases with different mechanisms of origin and pregnancy outcomes. Fertil Steril 2009, **92**：393.e5-9
13) Arizawa, M., Nakayama, M.：Suspected involvement of the X chromosome in placental mesenchymal dysplasia. Congenit Anom (Kyoto) 2002, **42**：309-317
14) Kotani, T., Sumigama, S., Tsuda, H. et al.：A case report of placental mesenchymal dysplasia with an increased VEGF-D expression. Placenta 2012, **33**：888-891
15) Heazell, A.E., Sahasrabudhe, N., Grossmith, A.K. et al.：A case of intrauterine growth restriction in association with placental mesenchymal dysplasia with abnormal placental lymphatic development. Placenta 2009, **30**：654-657

CLINICAL GENETICS An International Journal of Genetics, Molecular and Personalized Medicine

Clin Genet 2013

Published by John Wiley & Sons Ltd
CLINICAL GENETICS
doi: 10.1111/cge.12318

Short Report

A novel *de novo* point mutation of the OCT-binding site in the *IGF2/H19*-imprinting control region in a Beckwith–Wiedemann syndrome patient

Higashimoto K, Jozaki K, Kosho T, Matsubara K, Fuke T, Yamada D, Yatsuki H, Maeda T, Ohtsuka Y, Nishioka K, Joh K, Koseki H, Ogata T, Soejima H. A novel *de novo* point mutation of the OCT-binding site in the *IGF2/H19*-imprinting control region in a Beckwith–Wiedemann syndrome patient.
Clin Genet 2013. © John Wiley & Sons A/S. Published by John Wiley & Sons Ltd, 2013

The *IGF2/H19*-imprinting control region (ICR1) functions as an insulator to methylation-sensitive binding of CTCF protein, and regulates imprinted expression of *IGF2* and *H19* in a parental origin-specific manner. ICR1 methylation defects cause abnormal expression of imprinted genes, leading to Beckwith–Wiedemann syndrome (BWS) or Silver–Russell syndrome (SRS). Not only ICR1 microdeletions involving the CTCF-binding site, but also point mutations and a small deletion of the OCT-binding site have been shown to trigger methylation defects in BWS. Here, mutational analysis of ICR1 in 11 BWS and 12 SRS patients with ICR1 methylation defects revealed a novel *de novo* point mutation of the OCT-binding site on the maternal allele in one BWS patient. In BWS, all reported mutations and the small deletion of the OCT-binding site, including our case, have occurred within repeat A2. These findings indicate that the OCT-binding site is important for maintaining an unmethylated status of maternal ICR1 in early embryogenesis.

Conflict of interest

The authors have no competing financial interests to declare.

K Higashimoto[a], K Jozaki[a], T Kosho[b], K Matsubara[c], T Fuke[c], D Yamada[d], H Yatsuki[a], T Maeda[a], Y Ohtsuka[a], K Nishioka[a], K Joh[a], H Koseki[d], T Ogata[e] and H Soejima[a]

[a]Division of Molecular Genetics & Epigenetics, Department of Biomolecular Sciences, Faculty of Medicine, Saga University, Saga, Japan, [b]Department of Medical Genetics, Shinshu University School of Medicine, Matsumoto, Nagano, Japan, [c]Department of Molecular Endocrinology, National Research Institute for Child Health and Development, Tokyo, Japan, [d]Laboratory for Developmental Genetics, RIKEN Center for Integrative Medical Sciences (IMS), Yokohama, Kanagawa, Japan, and [e]Department of Pediatrics, Hamamatsu University School of Medicine, Hamamatsu, Japan

Key words: Beckwith–Wiedemann syndrome – ICR1 methylation defect – *IGF2/H19* – OCT-binding site – Silver–Russell syndrome

Corresponding author: Hidenobu Soejima, Division of Molecular Genetics & Epigenetics, Department of Biomolecular Sciences, Faculty of Medicine, Saga University, 5-1-1 Nabeshima, Saga 849–8501, Japan.
Tel.: +81 952 34 2260;
fax: +81 952 34 2067;
e-mail: soejimah@cc.saga-u.ac.jp

Received 5 August 2013, revised and accepted for publication 6 November 2013

Human 11p15 contains two neighboring imprinted domains, *IGF2/H19* and *KCNQ1*. Each domain is controlled by its own imprinting control region: ICR1 or ICR2, respectively (1). ICR1 methylation defects cause abnormal imprinted expression of insulin-like growth factor 2 (*IGF2*), which encodes a growth factor, and non-coding RNA *H19*, which possesses possible tumor-suppressor functions, leading to Beckwith–Wiedemann syndrome (BWS: OMIM 130650) and Silver–Russell syndrome (SRS: OMIM 180860), respectively (1, 2).

BWS is a congenital overgrowth disorder characterized by macroglossia, macrosomia, and abdominal wall defects, whereas SRS is a congenital growth retardation disorder characterized by a typical facial gestalt, clinodactyly V, and body asymmetry (1, 2). Among varied causative genetic and epigenetic abnormalities, ICR1 methylation defects are etiologies common to both diseases. Gain of methylation (GOM) and loss of methylation (LOM) at ICR1 account for ~5% of BWS and ~44% of SRS cases, respectively (1, 2).

ICR1 upstream of *H19* is a differentially methylated region (DMR) that is methylated exclusively on the paternal allele, and it regulates the imprinted expression of paternally expressed *IGF2* and maternally expressed *H19*. On the maternal allele, unmethylated ICR1 bound by CTCF forms a chromatin insulator that prevents *IGF2* promoter activation by the enhancer downstream of *H19*, resulting in silencing of *IGF2* and activation of *H19*. On the paternal allele, methylation-sensitive CTCF cannot bind to methylated ICR1, resulting in activation of *IGF2* and silencing of *H19* (3, 4). CTCF also maintains the unmethylated status of ICR1 on the maternal allele (5, 6).

Human ICR1 contains two different repetitive sequences (A and B) and seven CTCF-binding sites (CTSs) (Fig. 1a). A maternally inherited ICR1 microdeletion (1.4–2.2 kb), which affects ICR1 function and CTCF binding by changing CTS spacing, has been reported to result in ICR1-GOM in a few familial BWS cases (7–9). ICR1 also contains other protein-binding motifs, such as OCT, SOX, and ZFP57 (10, 11). Recently, point mutations and a small deletion of the OCT or SOX motif have been reported in a few BWS patients with ICR1-GOM (10, 12, 13).

Here, mutational analysis in 11 BWS and 12 SRS patients with ICR1 methylation defects revealed a novel *de novo* point mutation in the OCT-binding site on the maternal allele of one BWS patient.

Materials and methods

Patients

Eleven BWS and twelve SRS patients, who were clinically diagnosed, were enrolled in this study. All BWS and SRS patients displayed isolated GOM and LOM of ICR1, respectively. This study was approved by the Ethics Committee for Human Genome and Gene Analyses of the Faculty of Medicine, Saga University. Written informed consents were obtained from the parents or guardians of the patients.

Sequencing analysis of ICR1

A genomic region in and around ICR1, which included seven CTSs and three OCT-binding sites, was directly sequenced in all patients as previously described (14). All polymerase chain reaction (PCR) primer pairs used are listed in Table S1, Supporting Information.

Microsatellite analysis

For quantitative polymorphism analysis, tetranucleotide repeat markers, *D11S1984* at 11p15.5 and *D11S1997* at 11p15.4, were amplified and analyzed with GeneMapper software. The peak height ratios of the paternal allele to the maternal allele were calculated.

Southern blot analysis

Methylation-sensitive Southern blots with *Pst*I/*Mlu*I and *Bam*HI/*Not*I were employed for ICR1 and ICR2, respectively, as described previously (15). Band intensity was measured using a FLA-7000 fluoro-image analyzer (Fujifilm, Tokyo, Japan). The methylation index (MI, %) was then calculated.

Bisulfite sequencing

Bisulfite sequencing was performed covering the three variants within ICR1 that were found in BWS-s043. Genomic DNA was bisulfite-converted using an EpiTect Bisulfite Kit (Qiagen, Hilden, Germany). After PCR amplification, the products were cloned and sequenced.

Electrophoretic mobility shift assay

The pCMX-Flag-human OCT4 and pCMX-Flag-human SOX2 were simultaneously transfected into HEK293 cells. The nuclear extracts from HEK293 cells expressing human OCT4/SOX2 and mouse ES cells were used. Electrophoretic mobility shift assay (EMSA) was performed as described previously (10). For supershift analysis, 1.5 μg of anti-OCT4 antibody (Abcam, ab19857, Cambridge, UK) or 1.5 μg of anti-SOX2 antibody (R&D systems, AF2018, Minneapolis, MN) was used. The unlabeled probes were also used as competitors. The reaction mixtures were separated on a 4% polyacrylamide gel and exposed to a film. Oligonucleotide sequences are presented in Table S1.

Results

Among 11 BWS and 12 SRS patients with ICR1 methylation defects, 7 and 2 variants from 5 BWS and 2 SRS patients were found, respectively (Table 1). The variants in BWS-047 and BWS-s061 were polymorphisms. The remaining variants were not found in the normal population, the UCSC Genome Browser database, or the 1000 Genomes database, suggesting them to be candidates for causative mutations for ICR1 methylation defects. However, the positions of the variants, except

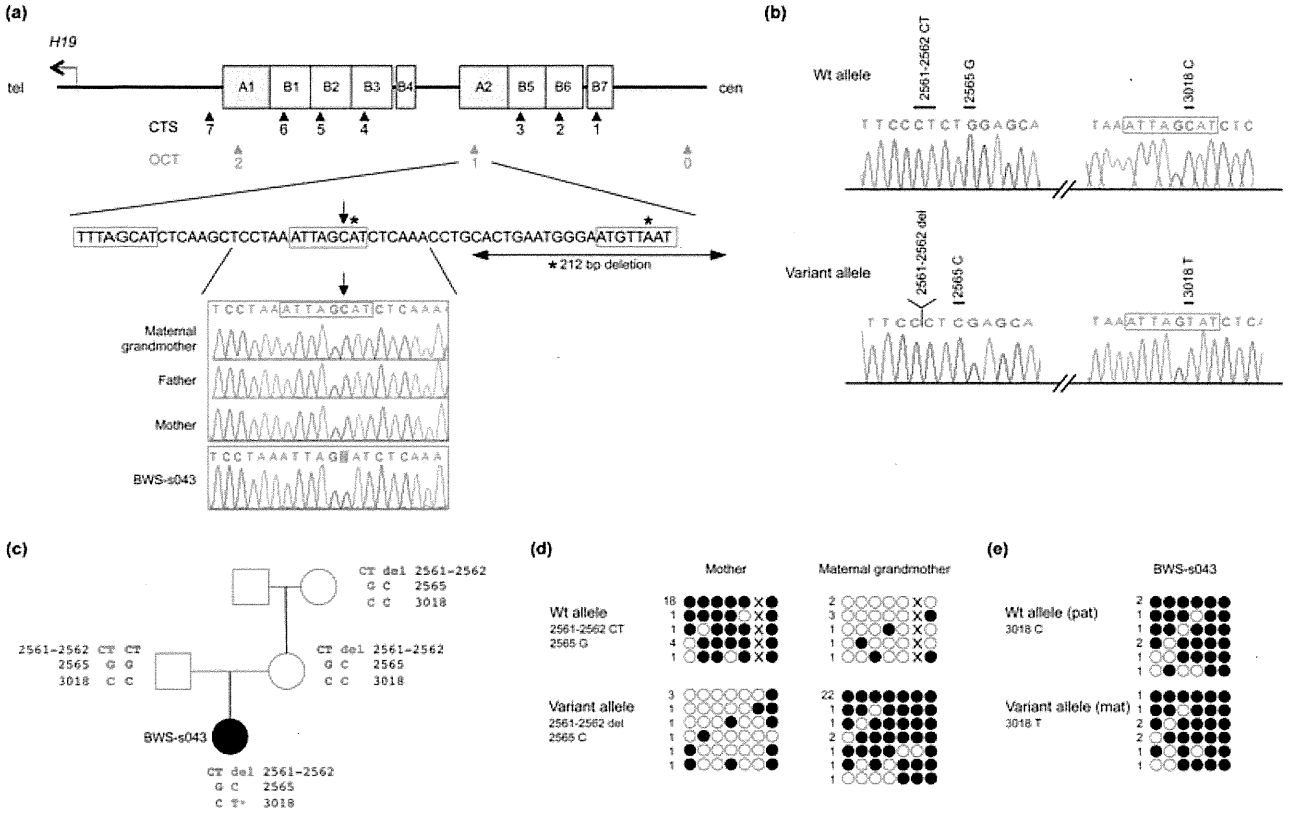

Fig. 1. The three variants in BWS-s043 and their effects on ICR1 methylation. (**a**) Map of ICR1 and the position of 2,023,018C>T. Upper panel: structure of ICR1. ICR1 consists of two repeat blocks. Each block consists of one repeat A and three or four repeat Bs. The black and red arrowheads indicate CTCF-binding sites (CTS) and OCT-binding sites (OCT), respectively. Middle panel: the position of 2,023,018C>T (arrow) and previously reported mutations and deletions (asterisks). Three octamer motifs are enclosed by a red line. Lower panel: electrophoretograms around 2,023,018C>T. BWS-s043 were heterozygous for the variant, whereas the maternal grandmother and both parents did not harbor it. (**b**) Haplotype encompassing the three variants in BWS-s043. Polymerase chain reaction (PCR) products encompassing the three variants were cloned and sequenced. All three variants were revealed to be on the same allele in BWS-s043. (**c**) Pedigree and haplotype of the family. Haplotype analysis showed that 2,023,018C>T (asterisk) occurred on the maternal allele in BWS-s043. (**d**) Bisulfite sequencing analysis encompassing the 2,022,561-562CT>delCT and the 2,022,565G>C variants in the mother and the maternal grandmother. Open and filled circles indicate unmethylated and methylated CpG sites, respectively. X indicates G at chr11: 2,022,565. Numerals on the left reflect the number of clones with the same methylation pattern. The variant allele was unmethylated in the mother and methylated in the maternal grandmother, respectively. (**e**) Bisulfite sequencing analysis encompassing 2,023,018C>T in BWS-s043. The maternal allele contained a *de novo* variant that was heavily methylated in BWS-s043, while differential methylation was maintained in other family members and normal controls without the variant (Fig. S2a).

Table 1. Variants found in this study[a]

Patient ID	MI of ICR1 (%)	Variant	Position (GRCh37/hg19 chr11)	Location	Transmission	Heterozygosity in normal population
BWS-047	100	G>Gdel	2,024,428	Centromeric outside of ICR1 (5′ of CTS1)	Maternal	2/116 (rs200288360)
		CT>CT del	2,022,561–2,022,562	Between A2 and B4	Maternal	na
BWS-s043	86	G>C	2,022,565	Between A2 and B4	Maternal	0/115
		C>T	2,023,018	A2 (OCT-binding site 1)	*De novo*	0/107
BWS-s061	76	C>T	2,023,497	B5 (5′ of CTS3)	Paternal	2/105
BWS-s081	67	C>T	2,025,777	Centromeric outside of ICR1 (3′ of OCT-binding site 0)	Paternal	0/106
BWS-s100	67	C>A	2,021,145	B1 (3′ of CTS6)	Maternal	0/105
SRS-002	4	G>Gdel	2,024,364	B7 (5′ of CTS1)	Unknown	0/106
SRS-s03	24	C>T	2,021,103	B1 (3′ of CTS6)	Maternal	0/106

ICR, imprinting control region; MI, methylation index; na, not analyzed.
[a]Parents' DNA were not available for SRS-002.

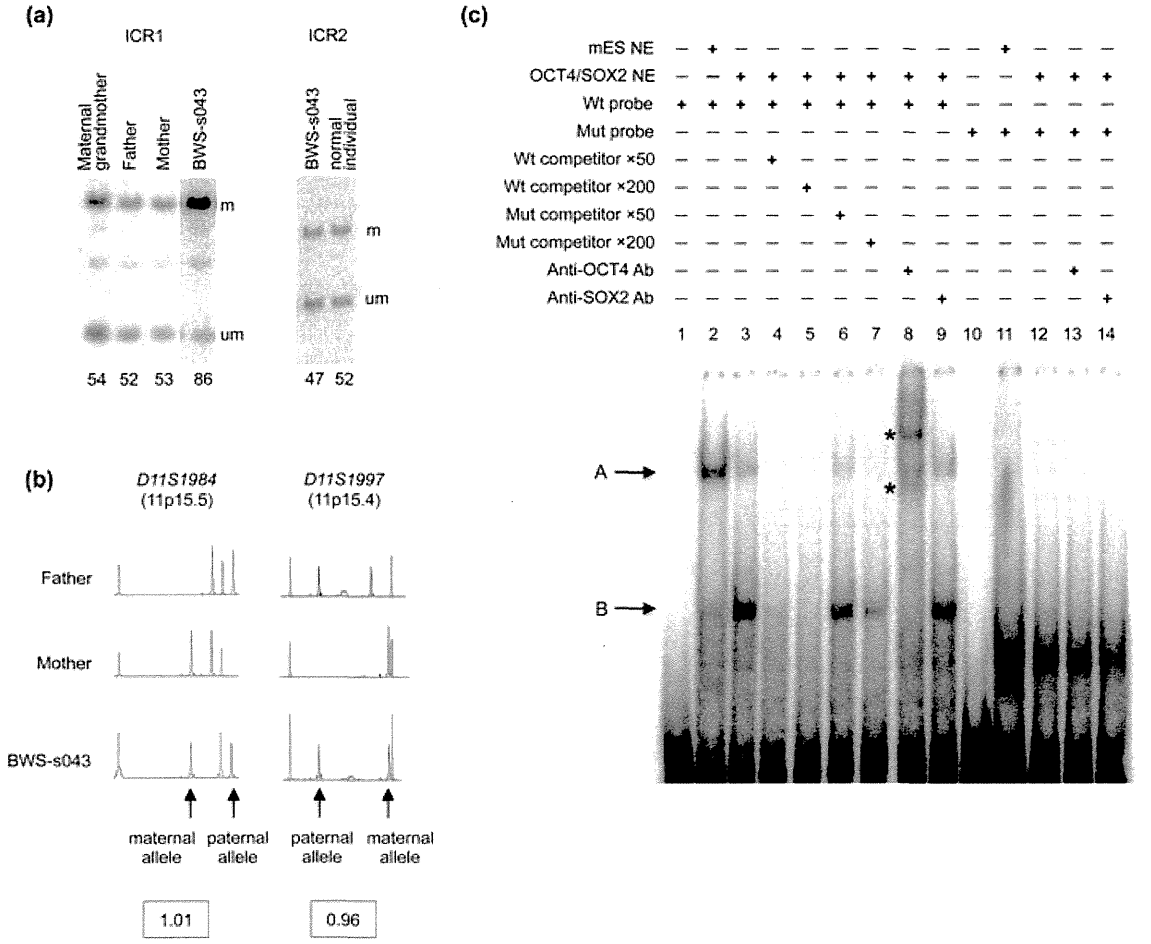

Fig. 2. Methylation-sensitive Southern blots and microsatellite analysis of BWS-s043, and electrophoretic mobility shift assay (EMSA) for 2,023,018C>T. (**a**) Methylation-sensitive Sothern blots of ICR1 and ICR2. Methylation indices [MI, %] are shown below each lane. MI was calculated using the equation $M/(M+U) \times 100$, where M is the intensity of the methylated band and U is the intensity of the unmethylated band. m, methylated band; um, unmethylated band. BWS-s043 showed ICR1-GOM, whereas the relatives did not. Methylation statuses of CTS1 and CTS4 are shown in Fig. S2b,c. Methylation of ICR2 in BWS-s043 was normal. (**b**) Microsatellite analysis at 11p15.4-p15.5. Ratios of the paternal allele to the maternal allele in BWS-s043 were approximately 1, indicating no uniparental disomy. Red peaks are molecular markers. (**c**) EMSA using the wild-type (Wt) probe and the mutant (Mut) probe encompassing 2,023,018C>T. The unlabeled Wt probe or Mut probe (×50 or ×200 molar excess) was used as a competitor. The arrows and asterisks indicate the protein-DNA complexes (A and B) and supershifted complexes, respectively. mES NE, nuclear extract from mouse ES cells; OCT4/SOX2 NE, nuclear extract from human HEK293 cells expressing OCT4/SOX2; Ab, antibody.

for BWS-s043, were not located at any protein-binding sites that have been reported as involved in methylation imprinting (CTCF, OCT, and ZFP57) (3, 4, 10, 12, 16). Furthermore, we did not find any protein-oligonucleotide complexes in EMSA using mouse ES nuclear extracts and oligonucleotide probes encompassing all variants, except for BWS-s043 (Fig. S1). Therefore, we analyzed further three variants in BWS-s043, which were in and around the OCT-binding site 1.

First, we re-confirmed that BWS-s043 showed GOM near CTS6 within ICR1, but it did not demonstrate LOM at ICR2, paternal uniparental disomy of chromosome 11, or a *CDKN1C* mutation (Fig. 2a,b, and data not shown). The 2,023,018C>T variant was located in the second octamer motif of OCT-binding site 1 within repeat A2 (Fig. 1a). The other two variants were located approximately 450 bp on the telomeric side of the 2,023,018C>T variant, between repeats A2 and B4 (Fig. 1a, Table 1). The 2,023,018C>T variant was absent in other family members, indicating a *de novo* variant (Fig. 1a). To clarify if the *de novo* variant in the patient occurred on the maternal or paternal allele, we performed haplotype analysis with PCR covering all three variants. We found all three variants were located on the same allele and the 2,023,018C>T variant occurred *de novo* on the maternal allele because the 2,022,561–562CT>delCT and 2,022,565G>C variants were on the maternal allele in the patient (Fig. 1b,c).

Next, we investigated the methylation status of ICR1. Methylation-sensitive Southern blots and bisulfite sequencing showed normal methylation of ICR1 in the parents and the maternal grandmother (Figs 2a and S2). As for the 2,022,561-562CT>delCT and the 2,022,565G>C variants, the variant allele was unmethylated in the mother, but methylated in the grandmother (Fig. 1d). On the basis of methylation

analysis, the variant allele in the grandmother must have been transmitted by her father, and that in the mother must have been transmitted by her mother. The results indicated that the variant allele could be either methylated or unmethylated during gametogenesis, strongly suggesting no relation between the variants and ICR1-GOM. On the other hand, bisulfite sequencing including the 2,023,018C>T variant revealed that both the variant and wild-type alleles were heavily methylated in the patient (Fig. 1e), while differential methylation was maintained in other family members and normal controls without the variant (Fig. S2a). As the *de novo* variant on the maternal allele was located within the OCT-binding site, which is required for the maintenance of the unmethylated status in a mouse model, the variant was likely involved in ICR1-GOM (17, 18).

Finally, we performed EMSA to determine if 2,023,018C>T influenced the binding ability of nuclear protein factors, such as OCT4 and SOX2 (Fig. 2c). The wild-type probe formed two complexes (A and B) with the nuclear extracts of mouse ES cells and HEK293 cells expressing OCT4/SOX2 (lanes 2 and 3), whereas such complexes were not observed in the mutant probe (lanes 11 and 12). Complexes A and B competed more efficiently with wild-type than with the mutant competitor (lanes 4 to 7). Furthermore, complex B, but not A, was supershifted with the antibody against OCT4 (lane 8). The supershift did not occur with the antibody against SOX2 and with both antibodies using the mutant probe (lanes 9, 13, and 14). These data demonstrated that 2,023,018C>T abrogated binding ability of a nuclear factor, most likely OCT4. Taken together, our data strongly suggest that 2,023,018C>T is a mutation that could prevent OCT4 binding to the OCT-binding site and induce ICR1-GOM, leading to BWS.

Discussion

We identified a novel *de novo* point mutation, chr11: 2,023,018C>T, in OCT-binding site 1 within repeat A2 in a BWS patient with ICR1-GOM. Our data strongly suggest the involvement of the mutation in GOM at ICR1. In a mouse cell model, the evolutionarily well-conserved dyad octamer motif within ICR1, which is bound by OCT protein, has been shown to be required for the maintenance of unmethylated status competing against *de novo* methylation (17). In addition, the importance of a SOX motif flanked by an OCT motif has also been reported (19). Recent studies have shown that the SOX–OCT motif functions to maintain unmethylated status *in vitro* and *in vivo*; a cooperative function of CTCF and OCT/SOX for maintenance of differential methylation has been suggested as responsible (18, 19). Although there is one OCT-binding site in mice, three evolutionarily conserved OCT-binding sites (0, 1, 2) are located in and around ICR1 in humans. As all mutations and the small deletion previously reported in addition to our case occurred in site 1 within repeat A2 (Fig. 1a), site 1 within repeat A2 likely plays a more important role for maintaining unmethylated status of maternal ICR1 in humans than the other OCT-binding sites (10, 12, 13).

ICR1-GOM cases, including ours, with mutations/deletions also show partial hypermethylation in spite of pre-existent genetic aberrations in the oocyte (9, 12, 13, 20), suggesting aberrant hypermethylation at ICR1 would also be stochastically acquired at a cellular level even in the existence of such aberrations.

As for SRS, including familial cases, the ICR1 mutation has not been found except in one sporadic case to date (10). We did not find any promising mutations in this study, suggesting the cause of ICR1 methylation defects to differ between SRS and BWS.

In conclusion, we identified a novel *de novo* point mutation of OCT-binding site 1 within repeat A2, a location suggested to play an important role for maintaining the unmethylated status of maternal ICR1 in humans, on the maternal allele in a BWS patient with ICR1-GOM. However, genetic aberrations of ICR1 explain only 20% of BWS cases with ICR1-GOM (10). As aberrant methylation may occur as a consequence of stochastic events or environmental influences irrespective of ICR1 mutations, unknown causes for ICR1 methylation defects should be clarified.

Supporting Information

The following Supporting information is available for this article:

Fig. S1. EMSA for all variants found in this study, except for those in BWS-047 and BWS-s061, using the nuclear extract from mouse ES cells. The variant in BWS-s081 was located outside of ICR1, and a CpG site within the probe sequence was mostly unmethylated in three normal controls (data not shown). Thus, an unmethylated probe was used for it. Since the variants in BWS-s100 and SRS-s03 were located 3′ of CTS6 and found on the maternal allele, unmethylated probes were used for them. As for the variant in SRS-002, it was located 5′ of CTS1 but its parental origin was unknown. Thus, both unmethylated and methylated probes were used for it. There was no difference between a wt-probe and a variant-probe in each variant except for the BWS-s043 mutation. A wt-probe for the BWS-s043 mutation formed two complexes, whereas such complexes were not observed with a probe for the mutation. These results suggested that only the BWS-s043 mutation affected the protein–DNA interaction (see text and Fig. 2c for details). WT, probe for the wild-type sequence; MUT, probe for the BWS-s043 mutation; VAR, probe for the variant sequence; um, unmethylated probe; me, methylated probe; mES NE, nuclear extract from mouse ES cells.
Fig. S2. Bisulfite sequencing of the region encompassing the 2,023,018 variant, CTS1, and CTS4. (**a**) Results for the 2,023,018 variant. In the healthy members of the BWS-s043 family, comprised of the maternal grandmother, mother, and father, showed differential methylation. Three normal controls also showed differential methylation. In particular, normal control 3 was heterozygous for a SNP (rs61520309) and showed differential methylation in an allele-dependent manner. Open and filled circles indicate unmethylated and methylated CpG sites, respectively. (**b**) Results for CTS1. Two normal controls that were heterozygous for a SNP (rs2525885) showed differential methylation. The healthy family members also showed differential methylation, whereas the patient, BWS-s043, showed aberrant hypermethylation. CpG sites within CTS1 are indicated by a short horizontal line. X indicates T of the SNP (rs2525885). (**c**) Results for CTS4. The healthy family members and two normal controls showed differential

methylation. Among them, the parents and two normal controls were heterozygous for a SNP (rs2525883). The patient, BWS-s043, showed aberrant hypermethylation. CpG sites within CTS4 were indicated by a short horizontal line. X indicates T of the SNP (rs2525883).
Table S1. PCR primers and oligonucleotide probes used in this study.

Additional Supporting information may be found in the online version of this article.

Acknowledgements

This study was supported, in part, by a Grant for Research on Intractable Diseases from the Ministry of Health, Labor, and Welfare; a Grant for Child Health and Development from the National Center for Child Health and Development; a Grant-in-Aid for Challenging Exploratory Research; and, a Grant-in-Aid for Scientific Research (C) from the Japan Society for the Promotion of Science.

References

1. Weksberg R, Shuman C, Beckwith JB. Beckwith–Wiedemann syndrome. Eur J Hum Genet 2010: 18: 8–14.
2. Gicquel C, Rossignol S, Cabrol S et al. Epimutation of the telomeric imprinting center region on chromosome 11p15 in Silver–Russell syndrome. Nat Genet 2005: 37: 1003–1007.
3. Bell AC, Felsenfeld G. Methylation of a CTCF-dependent boundary controls imprinted expression of the Igf2 gene. Nature 2000: 405: 482–485.
4. Hark AT, Schoenherr CJ, Katz DJ, Ingram RS, Levorse JM, Tilghman SM. CTCF mediates methylation-sensitive enhancer-blocking activity at the H19/Igf2 locus. Nature 2000: 405: 486–489.
5. Schoenherr CJ, Levorse JM, Tilghman SM. CTCF maintains differential methylation at the Igf2/H19 locus. Nat Genet 2003: 33: 66–69.
6. Pant V, Mariano P, Kanduri C et al. The nucleotides responsible for the direct physical contact between the chromatin insulator protein CTCF and the H19 imprinting control region manifest parent of origin-specific long-distance insulation and methylation-free domains. Genes Dev 2003: 17: 586–590.
7. Sparago A, Cerrato F, Vernucci M, Ferrero GB, Silengo MC, Riccio A. Microdeletions in the human H19 DMR result in loss of IGF2 imprinting and Beckwith–Wiedemann syndrome. Nat Genet 2004: 36: 958–960.
8. Prawitt D, Enklaar T, Gärtner-Rupprecht B et al. Microdeletion of target sites for insulator protein CTCF in a chromosome 11p15 imprinting center in Beckwith–Wiedemann syndrome and Wilms' tumor. Proc Natl Acad Sci U S A 2005: 102: 4085–4090.
9. Beygo J, Citro V, Sparago A et al. The molecular function and clinical phenotype of partial deletions of the IGF2/H19 imprinting control region depends on the spatial arrangement of the remaining CTCF-binding sites. Hum Mol Genet 2013: 22: 544–557.
10. Demars J, Shmela ME, Rossignol S et al. Analysis of the IGF2/H19 imprinting control region uncovers new genetic defects, including mutations of OCT-binding sequences, in patients with 11p15 fetal growth disorders. Hum Mol Genet 2010: 19: 803–814.
11. Quenneville S, Verde G, Corsinotti A et al. In embryonic stem cells, ZFP57/KAP1 recognize a methylated hexanucleotide to affect chromatin and DNA methylation of imprinting control regions. Mol Cell 2011: 44: 361–372.
12. Poole RL, Docherty LE, Al Sayegh A et al. Targeted methylation testing of a patient cohort broadens the epigenetic and clinical description of imprinting disorders. Am J Med Genet A 2013: 161: 2174–2182.
13. Berland S, Appelbäck M, Bruland O et al. Evidence for anticipation in Beckwith–Wiedemann syndrome. Eur J Hum Genet 2013: 21: 1344–1348.
14. Higashimoto K, Nakabayashi K, Yatsuki H et al. Aberrant methylation of H19-DMR acquired after implantation was dissimilar in soma versus placenta of patients with Beckwith–Wiedemann syndrome. Am J Med Genet A 2012: 158A: 1670–1675.
15. Soejima H, Nakagawachi T, Zhao W et al. Silencing of imprinted CDKN1C gene expression is associated with loss of CpG and histone H3 lysine 9 methylation at DMR-LIT1 in esophageal cancer. Oncogene 2004: 23: 4380–4388.
16. Mackay DJ, Callaway JL, Marks SM et al. Hypomethylation of multiple imprinted loci in individuals with transient neonatal diabetes is associated with mutations in ZFP57. Nat Genet 2008: 40: 949–951.
17. Hori N, Nakano H, Takeuchi T et al. A dyad Oct-binding sequence functions as a maintenance sequence for the unmethylated state within the H19/Igf2-imprinted control region. J Biol Chem 2002: 277: 27960–27967.
18. Sakaguchi R, Okamura E, Matsuzaki H, Fukamizu A, Tanimoto K. Sox-Oct motifs contribute to maintenance of the unmethylated H19 ICR in YAC transgenic mice. Hum Mol Genet 2013: 22: 4627–4637.
19. Hori N, Yamane M, Kouno K, Sato K. Induction of DNA demethylation depending on two sets of Sox2 and adjacent Oct3/4 binding sites (Sox-Oct motifs) within the mouse H19/insulin-like growth factor 2 (Igf2) imprinted control region. J Biol Chem 2012: 287: 44006–44016.
20. Sparago A, Russo S, Cerrato F et al. Mechanisms causing imprinting defects in familial Beckwith–Wiedemann syndrome with Wilms' tumour. Hum Mol Genet 2007: 16: 254–264.

Rumbajan et al. BMC Cancer 2013, 13:608
http://www.biomedcentral.com/1471-2407/13/608

BMC Cancer

RESEARCH ARTICLE Open Access

Comprehensive analyses of imprinted differentially methylated regions reveal epigenetic and genetic characteristics in hepatoblastoma

Janette Mareska Rumbajan[1,2], Toshiyuki Maeda[1], Ryota Souzaki[3], Kazumasa Mitsui[4], Ken Higashimoto[1], Kazuhiko Nakabayashi[5], Hitomi Yatsuki[1], Kenichi Nishioka[1], Ryoko Harada[4], Shigehisa Aoki[6], Kenichi Kohashi[7], Yoshinao Oda[7], Kenichiro Hata[5], Tsutomu Saji[4], Tomoaki Taguchi[3], Tatsuro Tajiri[8], Hidenobu Soejima[1*] and Keiichiro Joh[1*]

Abstract

Background: Aberrant methylation at imprinted differentially methylated regions (DMRs) in human 11p15.5 has been reported in many tumors including hepatoblastoma. However, the methylation status of imprinted DMRs in imprinted loci scattered through the human genome has not been analyzed yet in any tumors.

Methods: The methylation statuses of 33 imprinted DMRs were analyzed in 12 hepatoblastomas and adjacent normal liver tissue by MALDI-TOF MS and pyrosequencing. Uniparental disomy (UPD) and copy number abnormalities were investigated with DNA polymorphisms.

Results: Among 33 DMRs analyzed, 18 showed aberrant methylation in at least 1 tumor. There was large deviation in the incidence of aberrant methylation among the DMRs. *Kv*DMR1 and *IGF2*-DMR0 were the most frequently hypomethylated DMRs. *INPP5Fv2*-DMR and *RB1*-DMR were hypermethylated with high frequencies. Hypomethylation was observed at certain DMRs not only in tumors but also in a small number of adjacent histologically normal liver tissue, whereas hypermethylation was observed only in tumor samples. The methylation levels of long interspersed nuclear element-1 (LINE-1) did not show large differences between tumor tissue and normal liver controls. Chromosomal abnormalities were also found in some tumors. 11p15.5 and 20q13.3 loci showed the frequent occurrence of both genetic and epigenetic alterations.

Conclusions: Our analyses revealed tumor-specific aberrant hypermethylation at some imprinted DMRs in 12 hepatoblastomas with additional suggestion for the possibility of hypomethylation prior to tumor development. Some loci showed both genetic and epigenetic alterations with high frequencies. These findings will aid in understanding the development of hepatoblastoma.

Keywords: Hepatoblastoma, Genomic imprinting, Differentially methylated region, DNA methylation

Background

Hepatoblastoma is the most common primary liver tumor in children, accounting for just over 1% of pediatric cancers and 79% of liver cancers in children under the age of 15 [1]. Most of these tumors are purely derived from epithelium composed exclusively of immature hepatocytic elements, known as fetal and embryonal types. The fetal type consists of smaller than normal hepatocytes that are arranged in irregular laminae, recapitulating those of the fetal liver. The embryonal type is comprised of smaller cells as compared to the fetal type. It has a more immature appearance and pattern of growth. Some of the tumors, referred to as mixed type, are characterized by epithelial patterns and spindled mesenchymal cells. A much rarer variant of such mixed type tumor harbors teratoid features, which contains foci of mature cartilage, intestinal-type or keratinized epithelium, melanin pigment, or skeletal

* Correspondence: soejimah@cc.saga-u.ac.jp; joh@cc.saga-u.ac.jp
[1]Department of Biomolecular Sciences, Division of Molecular Genetics & Epigenetics, Faculty of Medicine, Saga University, Nabeshima 5-1-1, Saga 849-8501, Japan
Full list of author information is available at the end of the article

muscle in addition to the elements mentioned above. To date, several genetic and epigenetic features have been observed in hepatoblastoma (reviewed in [2]). The most recurrent cytogenetic abnormalities include the presence of extra copies of chromosomes 2, 8, 20, and the loss of chromosome 4. Mutations or upregulation of the genes involved in embryonic development have been reported. For example, *APC*, *CTNNB1*, *AXIN1*, and *AXIN2* (key factors involved in the Wnt signaling pathway) are frequently mutated, suggesting that aberration of this pathway occurs as an early event during tumorigenesis. Mutation of *PIK3CA*, amplification of *PIK3C2B*, and upregulation of hedgehog ligands and their target genes have also been reported. Epigenetic silencing by promoter hypermethylation occurs at several tumor suppressor genes, such as *SFRP1*, *APC*, *HHIP*, *SOCS1*, *CASP8*, and *RASSF1A*. In addition, several imprinted genes, including *IGF2*, *DLK1*, *PEG3*, *PEG10*, *MEG3*, and *NDN*, have been reported to be overexpressed in hepatoblastoma [2].

Imprinted genes are expressed in a parent-of-origin-specific manner. They are usually clustered in subchromosomal regions called imprinting domains. The human genome contains more than 30 imprinting domains (http://www.geneimprint.com). Imprinting domains have at least one DMR that are characterized by DNA methylation on one of the two parental alleles. There are maternally methylated DMRs and paternally methylated DMRs. In addition, two classes of imprinted DMRs, gametic and somatic, have been described. Gametic DMRs acquire methylation during gametogenesis and the methylation is maintained from zygote to somatic cells during all the developmental stages. Most gametic DMRs are known as imprinting control regions (ICRs) that regulate the imprinted expression of the genes in the domain. By contrast, methylations of somatic DMRs are established during early embryogenesis after fertilization under the control of nearby ICRs [3]. Somatic DMRs also regulate the expression of the imprinted genes.

Many imprinted genes regulate cell growth and differentiation, and, thus, disruption of imprinting, mainly due to aberrant DNA methylation at the responsible DMR, is implicated in pre- and/or post-natal growth disorders and in the pathogenesis of cancers [4]. For example, hypermethylation of *H19*-DMR, which is the ICR of the *IGF2*/*H19* imprinting domain at the 11p15.5 locus, is a cause of Beckwith-Wiedemann syndrome (BWS), the most common overgrowth syndrome characterized by occasional development of embryonal tumors, including hepatoblastoma [5]. The hypermethylation leading to biallelic expression of *IGF2* is seen in a range of tumors, also including hepatoblastoma [6,7]. The LOH of 11p15.5, especially the loss of the maternal allele, is found in approximately 20% of hepatoblastoma cases, and it is reported to be a risk factor for the relapse of this tumor [7,8]. Furthermore, several imprinted genes are overexpressed in hepatoblastoma as mentioned above. Thus, it is speculated that aberrant DNA methylation at imprinted DMRs is a key mechanism during malignant transformation of progenitor cells in a variety of tissues, including the liver [2,9]. However, the methylation status of imprinted DMRs scattered through the human genome has yet to be analyzed comprehensively in hepatoblastoma.

In this study, we performed comprehensive methylation analyses and polymorphism analyses of 33 imprinted DMRs in hepatoblastoma. We therefore describe some epigenetic and genetic characteristics of hepatoblastoma. These findings collectively aid in the understanding of the development of hepatoblastoma.

Methods

Samples

Twelve hepatoblastomas and their paired adjacent normal liver tissues were analyzed. Eleven sporadic hepatoblastoma samples (HB01 - HB11) were obtained from the Department of Pediatric Surgery, Faculty of Medicine, Kyushu University, Japan. One hepatoblastoma developed in a BWS patient (BWS109) was obtained from Toho University, Omori Medical Centre, Japan. Histochemical analyses of the tumor tissues indicated that the average of the tumor cell contents was approximately 70%. Ten of the patients were treated based on the Japanese Study Group for Pediatric Liver Tumor-2 (JPLT-2) protocol (HB08 and HB09 were not). Clinical information of the hepatoblastoma cases is shown in Table 1. Three livers (CL7, CL16, CBD1) were used as normal controls. CL7 (a 7-year-old who died from spinal muscular atrophy type I-C with chronic respiratory insufficiency) and CL16 (a 16-year-old who died after head trauma) were provided by the non-profit organization, Human & Animal Bridging Research Organization (Chiba, Japan). CBD1 (a 7-month-old who had congenital biliary dilatation) was obtained from the Department of Pediatric Surgery, Faculty of Medicine, Kyushu University. Written informed consents were obtained from the parents or the guardians of the participants, because the participants were children or dead. This study was approved by the Ethical Committee for Human Genome and Gene Analyses of the Faculty of Medicine, Saga University.

DNA isolation and bisulphite conversion

Genomic DNA was extracted from each sample using the QIAamp DNA Mini Kit (Qiagen, Germany) according to the manufacturer's instructions. One microgram of genomic DNA was subjected to bisulfite conversion using the EZ DNA Methylation Kit™ (Zymo Research, CA), and then the converted DNA was eluted in 100 μl of water.

Table 1 Clinical information of hepatoblastoma cases

Case	Sex/age[a]	Histology	PRETEXT	Preoperative chemotherapy[b]	POSTTEXT	Outcome	Other information
HB01	F/1y3m	Combined fetal and embryonal type	III	CITA4	III	Alive	
HB02	F/3y2m	Fetal type[c]	III	CITA4	III	Aive	
HB03	F/7y11m	Hepatoblastoma (NOS)[d]	III	CITA5	III	Alive	Small for gestational age
HB04	M/1y4m	Mixed epithelial and mesenchymal with teratoid feature[c]	IV	CITA4 + ITEC2	IV	Alive	
HB05	M/1y2m	Mixed epithelial and mesenchymal with teratoid feature	III	CITA5	II	Alive	
HB06	M/10m	Mixed epithelial and mesenchymal with teratoid feature	III	CITA4	III	Alive	
HB07	M/8m	Combined fetal and embryonal type	II	CITA2	II	Alive	
HB08	F/28d	Combined fetal and embryonal type	II			Alive	
HB09	M/1y6m	Combined fetal and embryonal type	II			Treatment related death	Small for gestational age
HB10	F/6y6m	Fetal type	II	CITA2	II	Alive	
HB11	F/3m	Combined fetal and embryonal type	IV	CITA7	III	Treatment related death	
BWS109	F/1y0m	Hepatoblastoma (NOS)[d]	IV,M(+)	CITA7 + ITEC1	IV	Alive	Beckwith-Wiedemann syndrome, liver transplantation at 1 year old

[a]age at diagnosis, [b]CITA: cisplatin-pirarubicin, ITEC: Ifosfamide, pirarubicin, etoposide, and carboplatin. The numerals indicate the cycle numbers of the chemotherapy. [c]difficult to diagnose due to chemotherapy, [d]not otherwise specified.

MALDI-TOF MS analysis

The methylation status of imprinted DMRs was screened by MALDI-TOF MS analysis with a MassARRAY system (Sequenom, CA) [10], according to the manufacturer's instructions. MALDI-TOF MS analysis produced signal pattern pairs indicative of non-methylated and methylated DNA. Epityper software analysis of the signals yielded the methylation index which ranged from 0 (no methylation) to 1 (full methylation) of each CpG unit, which contained one or more CpG sites measured as one unit in the MALDI-TOF MS analysis. Aberrant methylation of a CpG unit was defined as when the difference of methylation indexes between two samples exceeded 0.15, which was based on the fact that we have previously found that the differences of *H19*-DMR hypermethylation or *Kv*DMR1 hypomethylation in BWS patients were at least more than 0.15 (data not shown). Since analyzed DMRs included several CpG units, aberrant methylation of a DMR was defined as when more than 60% of total number of analyzed CpG units showed aberrant methylation (with the difference exceeding 0.15). We used CL7 and CBD1 as normal controls in MALDI-TOF MS analysis.

Pyrosequencing

Pyrosequencing was conducted using QIAGEN PyroMark Q24 according to the manufacturer's instruction (Qiagen, Germany). Some of the primers for DMR analysis were described by Woodfine et al. [11]. We designed other primers by using PyroMark Assay Design 2.0 (Qiagen, Germany). The primers for LINE-1 (GenBank accession no. X58075) analyses were described by Bollati et al. [12]. The criterion for MALDI-TOF MS analysis was also employed to define the aberrant methylation of each CpG site and an analyzed region. We used three livers, i.e. CL7, CL16, and CBD1, as normal controls in pyrosequencing. The control livers were analyzed in triplicate for LINE-1 and once for DMRs.

DNA Polymorphism analysis

LOH, UPD, and copy number abnormalities were investigated with DNA polymorphisms. For quantitative analyses, tetranucleotide repeat markers near the imprinted DMRs were amplified and separated by electrophoresis on an Applied Biosystems 3130 genetic analyzer. Data were then quantitatively analyzed with GeneMapper software (Applied Biosystems, CA). The peak height ratios of two parental alleles were calculated. A single nucleotide polymorphism (SNP) of *KCNQ1DN* (*rs229897*) was also analyzed.

All primers used in this study are shown in Additional file 1: Table S1.

Statistical analysis

The methylation statuses of the samples were compared in three pairs: adjacent normal liver tissue (A) and control livers (C), denoted as AxC; tumors (T) and control livers, denoted as TxC; tumors and adjacent normal liver tissue, denoted as TxA. The binomial distribution test was performed to compare aberrant hypomethylation and aberrant hypermethylation within each comparison pair (AxC, TxC, and TxA). The Chi squared test or Fisher's exact test was used for comparison between maternally methylated and paternally methylated DMRs and between gametic and somatic DMRs in aberrant hypomethylation and aberrant hypermethylation cases for each comparison pair. For LINE-1 methylation, a paired *t*-test was used to compare tumor and adjacent normal liver tissue, and an independent *t*-test (Welch's *t*-test) was used for comparing tumor or adjacent normal liver tissue with control liver. A p-value less than 0.05 was considered to be statistically significant. Bonferroni correction was performed when needed.

Results

Clinical information of hepatoblastoma cases

Clinical information of the 12 hepatoblastoma cases analyzed in this study are shown in Table 1. Eleven tumors were sporadic (HB01-HB11), and one was associated with BWS (BWS109). The ratio of males to females was 5:7. The mean age at diagnosis was 25.7 months, ranging from 28 days to 7 years and 11 months. In terms of histological features, 5 cases had combined fetal and embryonal types, 3 cases had mixed epithelial and mesenchymal features with teratoid features, 2 cases were fetal types, and 2 cases were hepatoblastomas (not otherwise specified). Using PRETEXT staging [13], 4 cases were stage II, 5 cases were stage III, and 3 cases were stage IV. Ten of twelve cases were undergoing chemotherapy based on the JPLT-2 protocol, but only two cases (HB05 and HB11) regressed to a lower stage after chemotherapy.

Analyses of aberrant methylation and genetic alterations at imprinted DMRs

We selected 33 regions reported previously as imprinted DMRs in the human genome [11,14] (refer to http://www.geneimprint.com/). Our strategy in this study involved screening the methylation levels of DMRs in tumors, their paired adjacent normal tissues, and normal control livers by MALDI-TOF MS. The samples that showed aberrant methylation were analyzed again by pyrosequencing to confirm the result. These two methods are the most reliable methods of methylation analysis at present [10,15,16]. First, we analyzed the methylation level of these regions in two normal livers, i.e. CL7 and CBD1, by MALDI-TOF MS (Additional file 2: Figure S1). A total

of 20 DMRs showed almost 50% methylation, however, 8 DMRs (*IGF2R*-DMR2, *IGF2*-DMR0, *IGF2*-DMR2, IG-DMR-CG4, IG-DMR-CG6, *TCEB3C*-DMR, *USP29*-DMR, and *NNAT*-DMR) showed mostly full methylation, and 5 DMRs (*TP73*-DMR, *SPTBN1*-DMR, *WT1-AS*-DMR, *DLK1*-DMR, and *GNASXL*-DMR) showed mostly no methylation. It is highly possible that these regions were not differentially methylated in the normal liver, probably due to tissue-specific and/or age-related features of differential methylation, because most of the regions were also analyzed by pyrosequencing and their methylation statuses were confirmed (Additional file 2: Figure S1).

Next, we screened the methylation status of the 33 DMRs in 12 hepatoblastomas and their paired adjacent normal liver tissue by MALDI-TOF MS. We found aberrant methylation in tumors and also in adjacent liver tissue by comparing the methylation between tumors and normal controls (TxC), tumors and adjacent liver tissue (TxA), and adjacent liver tissue and normal controls (AxC). The definition of aberrant methylation is described in the Methods section. After excluding samples harboring chromosomal abnormalities as described later, we confirmed the aberrant methylation using pyrosequencing, except in the case of *H19*-DMR (representative data is shown in Figure 1 and all data in Additional file 3: Figure S2). Additional normal control liver, CL16, was used in pyrosequencing analyses. The methylation status of *H19*-DMR was analyzed by hot-stop combined bisulfite restriction analysis (COBRA) [17] or bisulfite sequencing because of the difficulty in the primer-design for pyrosequencing (Additional file 4: Figure S3).

In order to exclude aberrantly methylated DMRs, as associated with chromosome abnormalities, such as UPD or copy number abnormality, DNA polymorphism analyses using microsatellites and SNPs were performed on all regions showing aberrant methylation in the MALDI-TOF MS analyses. We found seven genetic alterations in four tumors resulting in aberrant methylation: abnormal allelic copy number of 11p13-p15.5 in HB01, 20q11-q13 in HB05, and 19q13 and 20q13 in HB11; LOH of 7q32.2 and 11p15.5 in HB11; and paternal UPD of 11p13-p15.5 in BWS109 (Figure 2). We speculated the allelic imbalance statuses of these loci according to the results of MALDI-TOF MS analysis and DNA polymorphism analysis (Additional file 5: Figure S4). HB01 would harbor more paternal copies than the maternal copies in 11p13-p15.5. An abnormal allelic copy number of 20q11-q13 in HB05 would represent a higher copy number in the maternal allele than the paternal allele. HB11 would have more maternal copies of 19q13 and more paternal

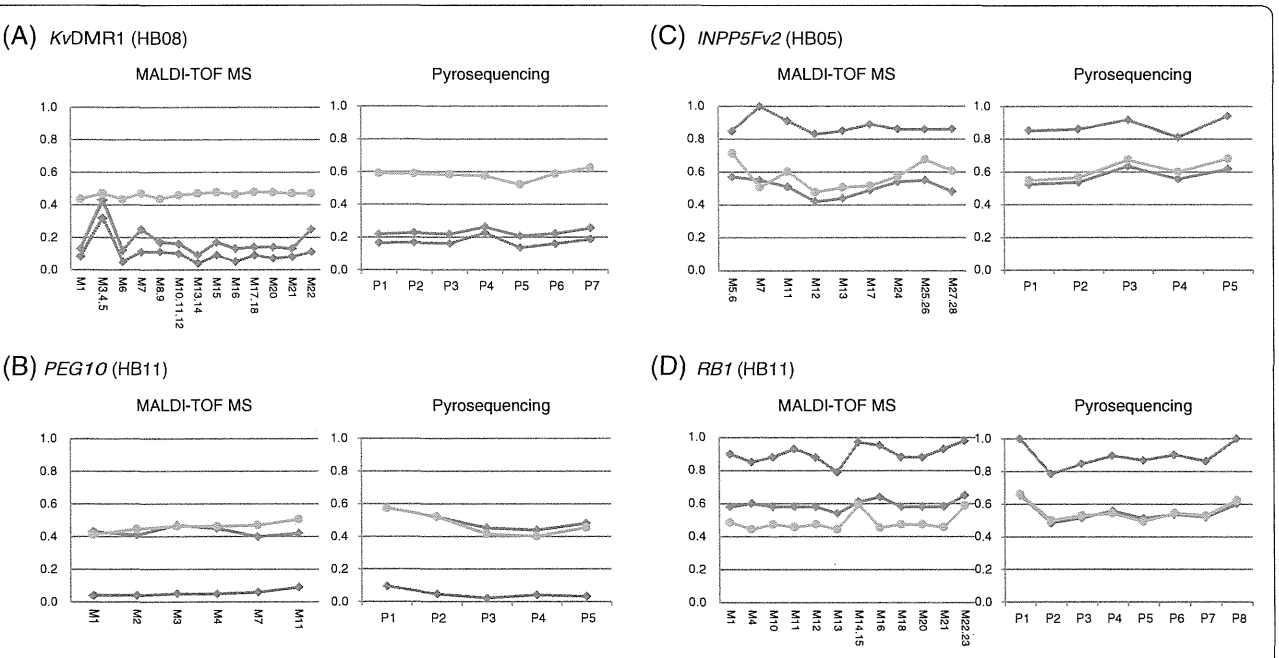

Figure 1 Representative results of methylation analyses by MALDI-TOF MS and pyrosequencing. (A and B) Representative samples of aberrant hypomethylation. *Kv*DMR1 of HB08 and PEG10 of HB11 are shown. *Kv*DMR1 was hypomethylated in both adjacent normal liver and tumor tissues, whereas *PEG10*-DMR was hypomethylated only in tumor tissue. **(C and D)** Representative samples of aberrant hypermethylation. *INPP5Fv2*-DMR in HB05 and *RB1*-DMR in HB11 are shown. Only tumors showed hypermethylation at these DMRs. Aberrant methylation of a DMR was defined as when more than 60% of total CpG units or CpG sites were aberrantly methylated. Aberrant methylation of a CpG unit or CpG site was defined as occurring when the difference of its methylation indexes in two samples exceeded 0.15. The vertical axis represents the methylation index; the horizontal axis represents CpG units (MALDI-TOF MS) or CpG sites (pyrosequencing) analyzed. Green line: average of normal control livers; blue line: adjacent normal liver; red line: tumor (hepatoblastoma).

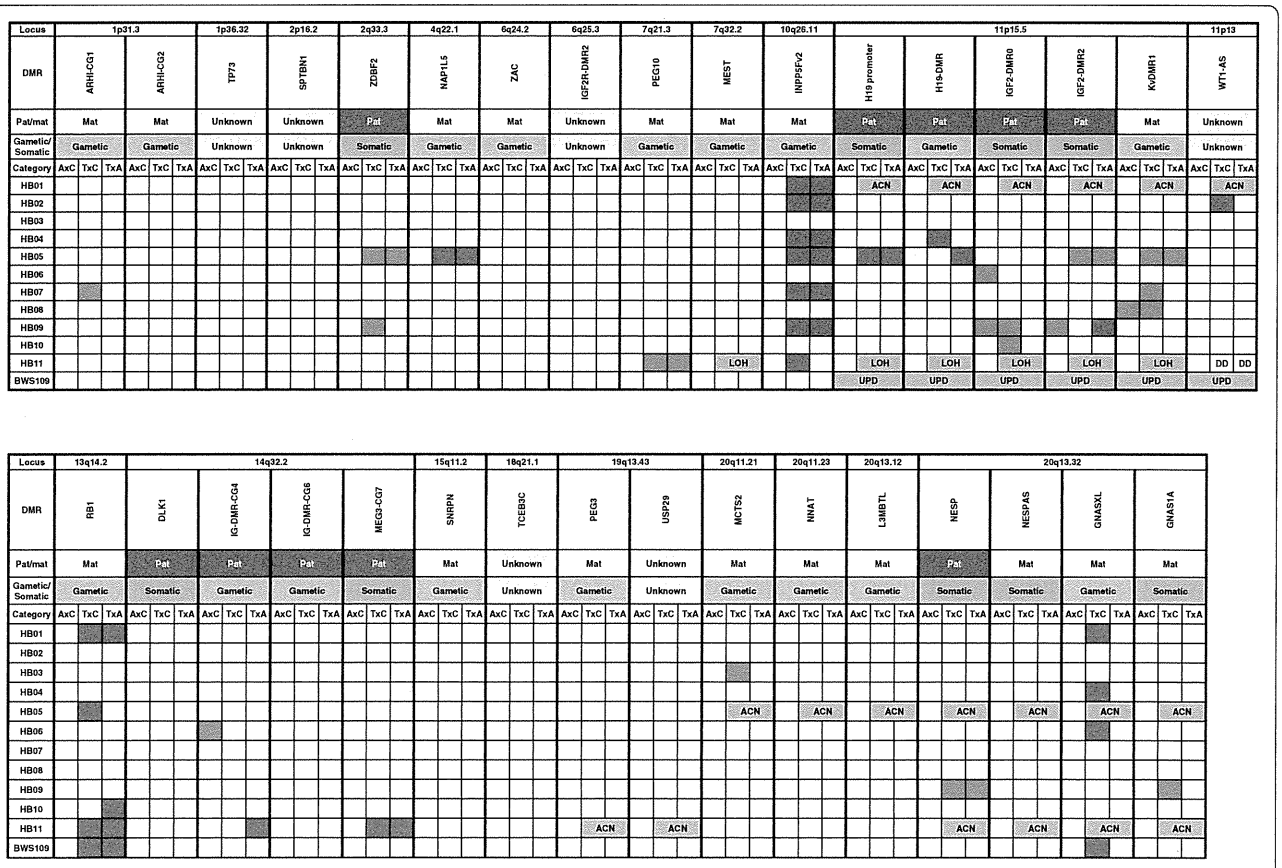

Figure 2 Aberrant methylations and genetic alterations of 33 imprinted DMRs in 12 hepatoblastomas. Aberrant hypomethylation and aberrant hypermethylation found in each comparison are indicated by blue and red boxes, respectively. Aberrant methylation was identified by comparing adjacent normal liver tissue with normal control livers: AxC; tumors compared with normal control livers: TxC; and tumors compared with adjacent normal livers: TxA. The classes of these DMRs in previous reports are shown in Pat/Mat and Gametic/Somatic rows. *ZDBF2*-DMR was tentatively assigned as a somatic DMR based on experiments from mice [35]. MALDI-TOF MS revealed that 13 DMRs, such as *TP73*-DMR, *SPTBN1*-DMR, *IGF2R*-DMR2, *IGF2*-DMR0, *IGF2*-DMR2, *WT1-AS*-DMR, *DLK1*-DMR, IG-DMR-CG4, IG-DMR-CG6, *TCEB3C*-DMR, *USP29*-DMR, *NNAT*-DMR, and *GNASXL*-DMR did not show differential methylation in control livers. Most of these methylation statuses were confirmed by pyrosequencing analysis. Mat: maternally methylated DMR; Pat: paternally methylated DMR; gametic: gametic DMR; somatic: somatic DMR. ACN: abnormal copy number; LOH: loss of heterozygosity; UPD: paternal uniparental disomy; DD: difficult to decide.

copies of 20q13. LOH of 7q32.2 and 11p15.5 would have occurred due to a paternal deletion and a maternal deletion, respectively. The paternal UPD was confirmed using the parents' DNA (Additional file 5: Figure S4). The extent of the UPD was found to be at 11p11.2–pter by a SNP array analysis (data not shown).

The following results described are shown in Figure 2. All tumors carried aberrant methylation in at least one DMR. HB05 carried aberrant methylations at 8 DMRs, the highest number of aberrant methylations, whereas HB03 and HB08 carried aberrant methylations at only one DMR, *MCTS2*-DMR and *Kv*DMR1, respectively. A total of 18 of 33 DMRs showed aberrant methylation, whereas 15 DMRs did not show such features in any tumors. There was large deviation in the incidence of aberrant methylation among the DMRs. *Kv*DMR1 and *IGF2*-DMR0 were the most frequently hypomethylated DMRs in 3 of 9 tumors. The most frequently hypermethylated DMR was *INPP5Fv2*-DMR, which occurred in 7 of 12 samples. *RB1*-DMR was also hypermethylated with a high frequency, which occurred in 5 of 12 samples. In addition, *GNASXL*-DMR was hypermethylated in 4 of 10 samples. The following DMRs showed aberrant methylation in only one tumor: *ARH1*-CG1, *NAP1L5*-DMR, *PEG10*-DMR, *H19* promoter, *WT1-AS*-DMR, *MEG3-CG7*-DMR, *MCTS2*-DMR, *NESP*-DMR, and *GNAS1A*-DMR.

Two chromosomal loci, 11p15.5 and 20q13.32, showed high frequencies of genetic and epigenetic alterations at 10 of 12 and 7 of 12, respectively. In the 11p15.5 locus, seven tumors carried the aberrant methylation and three samples carried genetic alterations. In the 20q13.32 locus, five tumors carried aberrant methylation and two carried an abnormal allelic copy number.

Comparisons of aberrantly methylated DMRs

We compared the numbers of aberrantly hypomethylated and hypermethylated DMRs in three pairs of the sample groups (Figure 3A). We excluded the DMRs harboring UPD or copy number abnormalities for the statistical analyses. Comparing adjacent normal liver tissues (A) and control livers (C), herein denoted as AxC, only hypomethylation was observed in adjacent normal liver tissue ($p = 0.031$). In the TxC comparison, both hypermethylation and hypomethylation were observed in tumors (no significant difference). In the TxA comparison, hypermethylation was observed more frequently than hypomethylation with statistical significance ($p = 0.013$). In addition, the number of hypomethylated DMRs in tumors was higher than that of adjacent normal liver tissue ($p = 0.040$), although Bonferroni correction did not show statistical significance of the difference with a significance level of 0.05/3 (approximately 0.0167). These results suggested a possibility that hypomethylation occurred at certain DMRs in adjacent normal liver tissue prior to tumor development, whereas hypermethylation occurred only within the tumor tissue itself.

We further compared the frequencies of aberrant methylation between paternally methylated DMRs and maternally methylated DMRs. As for hypomethylation, there was no significant difference between the two kinds of DMRs in each comparison (Figure 3B, left panel). In contrast, hypermethylation, which was observed only in tumors, tended to occur more frequently at maternally methylated DMRs than paternally methylated DMRs in the TxC comparison

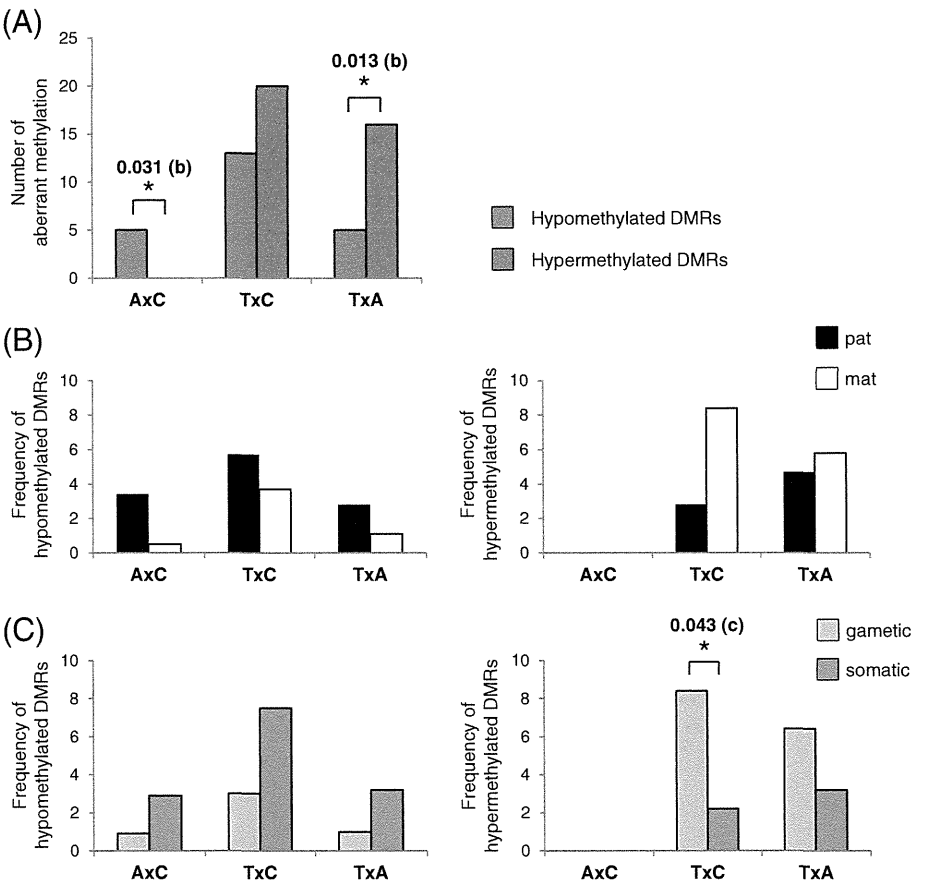

Figure 3 Comparison of aberrant methylations of DMRs in hepatoblastoma. (A) Comparison of the numbers of aberrantly hypomethylated (blue bars) and hypermethylated (red bars) DMRs. Hypomethylation, but not hypermethlation, was observed in adjacent normal tissues. Hypermethylation was observed more frequently than hypomethylation in tumors compared to adjacent normal tissues. **(B)** Comparison of the frequencies of aberrant methylations between the paternally methylated DMRs (black bars) and the maternally methylated DMRs (white bars). Left and right panels indicate hypomethylation and hypermethylation, respectively. There was no significant difference in both hypomethylation and hypermethylation. **(C)** Comparison of the frequencies of aberrant methylations between gametic DMRs (yellow bars) and somatic DMRs (green bars). Left and right panels indicate hypomethylation and hypermethylation, respectively. Hypermethylation was observed more frequently at gametic DMRs with statistically significant difference in tumors compared to control livers. The frequencies were compared in **(B)** and **(C)** because of the difference in the total numbers of DMRs in the two categories compared; that is, the paternal and the maternal DMRs or the gametic and the somatic DMRs. The asterisks indicated significant difference. The p values are shown above the comparisons. b: binomial test, c: chi squared test.

(p = 0.060) (Figure 3B, right panel). We also compared the frequencies of aberrant methylation between gametic DMRs and somatic DMRs. No significant difference in hypomethylation was found between the two kinds of DMRs in each comparison (Figure 3C, left panel). In contrast to hypomethylation, hypermethylation occurred at gametic DMRs more frequently with statistical significance (p = 0.043) (Figure 3C, right panel). This difference was mainly due to the frequent occurrence of hypermethylation at three maternally methylated and gametic DMRs, such as *INPP5Fv2*-DMR, *RB1*-DMR, and *GNASXL*-DMR (Figure 2).

Methylation status of LINE-1 in hepatoblastoma

We analyzed the methylation status of LINE-1 in all samples by pyrosequencing to assess the genome-wide methylation level. LINE-1 is a human repetitive element and constitutes approximately 30% of the human genome [18]. Its methylation status has been used as a surrogate marker for genome-wide DNA hypomethylation in many cancers [19,20]. We analyzed the methylation of four CpG sites in a LINE-1 sequence that were hypomethylated in cancers [21,22]. We compared the methylation levels of each CpG site among the three groups using Bonferroni correction with significance level of 0.0167 (Figure 4). Tumors showed slight hypomethylation only at CpG1 among four CpGs (p = 0.015 in TxA). However, other CpG sites did not show hypomethylation although bare hypermethylations (less than 2.5%) was found only in adjacent normal liver tissues at CpG2 (p = 0.001 in AxC and p = 0.010 in AxT). These results suggested that the genome-wide methylation levels were almost same among three sample groups.

Discussion

In this study, we found many imprinted DMRs methylated aberrantly in hepatoblastomas and paired adjacent normal liver tissue. An important finding was that the aberrant hypomethylation occurred not only in tumor tissue but also in adjacent normal liver tissue. One possible explanation is that the occurrence of the aberrant hypomethylation at certain DMRs may be a very early and specific event prior to tumor development, although there is another possibility that the tumor may induce methylation changes in the adjacent tissues. Okamoto et al. have previously reported a similar phenomenon with respect to aberrant hypermethylation of *H19*-DMR that was frequently found in normal tissues adjacent to Wilms' tumors, which carried the same aberrant methylation [23]. Based on the results, it was hypothesized that the preceding aberrant methylation may be a constitutional aberration in the onset of embryonal tumors. In contrast to the hypomethylation, the aberrant hypermethylation of the DMR occurred only in tumors. These results indicated that the hypermethylation of the DMRs, especially for *INPP5Fv2*-DMR, *RB1*-DMR, and *GNASXL*-DMR, was a specific event for tumor development; this suggested that the pre-cancerous cells did not carry hypermethylation at the DMRs, but acquired the aberrant methylation during tumor development.

We also analyzed the genome-wide methylation level, represented by LINE-1 methylation, and we did not find large difference among three sample groups as a

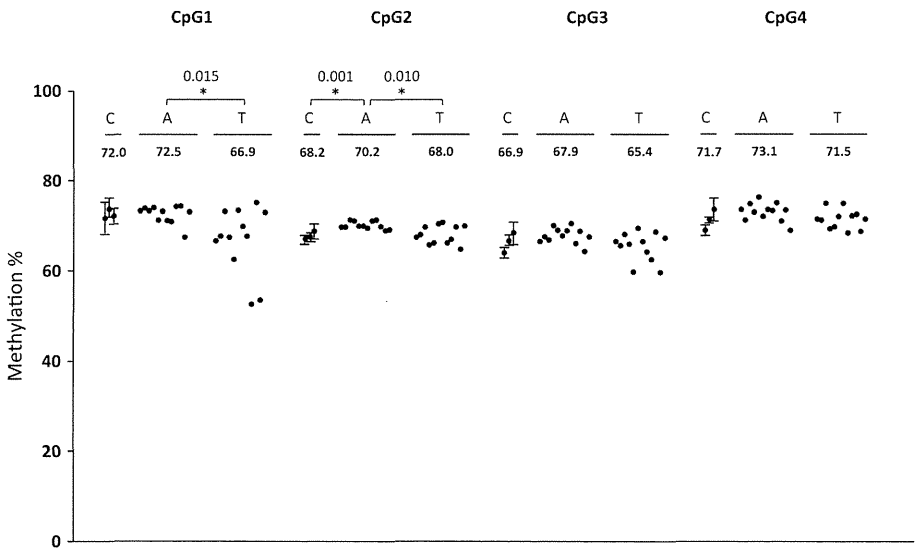

Figure 4 Methylation status of LINE-1. Methylation levels of four successive CpG sites in LINE-1 were analyzed in hepatoblastomas (T), paired adjacent normal liver tissues (A), and three normal control livers (C) by pyrosequencing. The normal controls were analyzed in triplicate and the average values were plotted with standard deviations. The average values of methylation (%) are shown for each sample groups. The asterisks indicated significant differences (p < 0.0167). Bonfferoni correction was applied for this statistical analysis.

whole. LINE-1 is usually hypomethylated in many adult tumors, and its methylation level correlates with clinicopathological features of the tumors [19]. The different situation concerning LINE-1 methylation between hepatoblastoma and adult tumors may reflect a different mechanism of tumorigenesis in embryonal tumors as compared to adult tumors.

Hypermethylation in tumors was frequently observed at three DMRs, *INPPF5v2*-DMR, *RB1*-DMR, and *GNASXL*-DMR. *INPPF5v2*-DMR controls the expression of *INPP5F* transcript variant 2, which encodes a protein of an unknown function [24,25]. *RB1*-DMR, located in intron 2 of the *RB1* gene, leads to maternal expression of transcript variants from exon 2B with very low expression in normal tissues [26]. The function of the variants in cell proliferation is not known. Thus, the effect of these hypermethylated DMRs on tumorigenesis would be little or unknown. *GNASXL*-DMR is associated with the paternal expression of *GNASXL*, which encodes a protein involved in signal transduction [27-29]. The DMR was shown to be mostly unmethylated in control livers (Additional file 2: Figure S1). Thus, hypermethylation of GNASXL-DMR would reduce expression of *GNASXL*. Unfortunately, the expression of genes linked to aberrantly methylated DMRs could not be analyzed due to poor RNA quality, which was probably due to effects of chemotherapy and a limited amount of samples. Therefore, we could not assess the involvement of hypermethylation in tumorigenesis of hepatoblastoma.

Another important finding was the frequent occurrence of both genetic and epigenetic alterations at the two chromosomal loci, 11p15.5 and 20q13.3. The 11p15.5 locus is a well-known imprinted locus responsible for BWS, a tumor-predisposing imprinting disorder. The locus was found to be altered genetically and/or epigenetically in 10 of 12 tumors. Hypermethylation at *H19*-DMR and hypomethylation at *IGF2*-DMR0 associated with biallelic expression of *IGF2* were reported in adult and embryological tumors, including hepatoblastoma [6,7]. Hypermethylation at *H19*-DMR and the *H19* promoter also reduced the expression of *H19* in Wilms' tumor [30,31]. In addition to epigenetic alterations, genetic alterations, such as the amplification of paternal alleles leading to overexpression of *IGF2* and LOH of the maternal allele leading to reduced expression of *H19*, were observed in sporadic Wilms' tumors [32,33]. In this study, in addition to the hypermethylations at *H19*-DMR and the *H19* promoter in two tumors, hypomethylation at *IGF2*-DMR0 occurred in another two adjacent normal liver tissues. Further, abnormal allelic copy number, paternal UPD, and maternal LOH of 11p15.5 were observed. The overexpression of *IGF2* and the reduced expression of *H19* would play an important role in tumorigenesis of hepatoblastoma.

The 20q13.3 locus was also altered genetically and/or epigenetically in 7 of 12 tumors. This locus is responsible for pseudohypoparathyroidism, a condition in which pathogenesis is attributed to the tissue specific imprinting of *Gsα*, for example, which occurs in the proximal renal tubule. On the other hand, an extra copy of chromosome 20 has been known to be the most recurrent cytogenetic alteration in hepatoblastoma [2,34]. We found copy number differences of the alleles in this region, suggesting the existence of non-imprinted oncogenic gene(s) in this region.

Many epigenetic and genetic alterations were found at the loci linked to the 33 imprinted DMRs in 12 hepatoblastomas. However, since sample numbers in this study were small, more hepatoblastoma samples should be analyzed to confirm the present data and to evaluate the precise role of these alterations in tumorigenesis in addition to assessing their usefulness as markers for clinical characteristics, such as stage classification, response to chemotherapy, and prognosis. Also needed are the expression analyses of the genes linked to aberrantly methylated DMRs to assess their role in tumor development, although it is very difficult to obtain hepatoblastoma samples without any chemotherapeutic history.

Conclusions

We found epigenetic and genetic characteristics of hepatoblastoma by comprehensive epigenetic and genetic analyses of 33 DMRs linked to imprinting loci in 12 hepatoblastoma samples and their adjacent normal liver tissues. These included aberrant hypomethylation in adjacent normal liver tissue, tumor-specific hypermethylation, and the frequent occurrence of both genetic and epigenetic alterations at 11p15.5 and 20q13.3 loci. Further studies using more hepatoblastoma samples are needed to confirm the present results and evaluate their roles in the tumor development.

Additional files

Additional file 1: Table S1. Primers used for this study.

Additional file 2: Figure S1. Maps of DMRs analyzed in this study and their methylation status in normal control livers. Upper part; The arrow represents the position and the direction of the transcription start site (TSS). P: promoter; Cen: centromere; Tel: telomere; yellow box (CGI): CpG island; orange boxes (M): CpG sites analyzed by MALDI-TOF MS; green boxes (P): CpG sites analyzed by pyrosequencing. Numbers with diagonal lines indicate CpG units (MALDI-TOF MS) or CpG sites (pyrosequencing), which could not be analyzed. Figures are not drawn to scale. Lower part; Results of MALDI-TOF MS and pyrosequencing are shown. In methylation graphs, the vertical axis represents the methylation index (0: no methylation; 1: full methylation). The horizontal axis represents CpG units or CpG sites. CL7 was analyzed in duplicate by MALDI-TOF MS analysis. Blue and red lines: CL7; green line: CBD1; dark grey line: CL16.

Additional file 3: Figure S2. Methylation data of the aberrantly methylated DMRs in hepatoblastomas. The results of MALDI-TOF MS (left panel) and pyrosequencing (right panel) are shown. The vertical axis represents the methylation index (0–1); the horizontal axis represents

CpG units (MALDI-TOF MS) or CpG sites (pyrosequencing). Green line: average of control livers; blue line: adjacent normal liver; red line: tumor (hepatoblastoma).

Additional file 4: Figure S3. Methylation status of *H19*-DMR as determined by bisulphite cloning sequencing and hot-stop COBRA. (A) Bisulphite sequencing of HB05, which was heterozygous for *rs2071094*. Filled circle: methylated CpG site; open circle: unmethylated CpG site. *rs2071094*: single nucleotide polymorphisms (A/T). CTCF6: CTCF binding site 6. *TaqI*: *TaqI* site used for hot-stop COBRA. (B) Hot-stop COBRA. End-labeled PCR products were obtained by PCR with ^{32}P labeled reverse primer in the final amplification cycle. The PCR products were digested with *TaqI* overnight and then electrophoresed. Band intensities were quantitated using the FLA-7000 fluoro-image analyzer (Fujifilm, Japan). un: unmethylated control DNA; me: fully methylated control DNA.

Additional file 5: Figure S4. Genetic alterations in hepatoblastoma. (A) Map of 11p15-p13 is shown uppermost. Black box: microsatellite marker; white box: DMR analyzed. Tel: telomere; Cen: centromere. Figure is not drawn to scale. Below the map, the representative data of the methylation analyses and microsatellite analyses are shown for three hepatoblastomas. For HB01 tumor, a high paternal copy number was estimated because of the hypermethylation at the paternally methylated *H19*-DMR and the hypomethylation at the maternally methylated *Kv*DMR1. LOH in HB11 tumor was indicated by the near loss of one of two alleles. The maternal allele could have been lost because of hypermethylation at *H19*-DMR and hypomethylation at *Kv*DMR1. The deviation of the allelic ratio in adjacent normal liver and tumor tissue indicates paternal UPD mosaicism in BWS109, whereas the allelic ratios in the parental blood were approximately 1. The level of mosaicism was higher in tumor than in adjacent normal liver tissue. In tumor samples, the value of the higher peak was divided by that of the lower peak. In adjacent normal liver and parental samples, the ratios were calculated following the pattern in their related tumor. (B) LOH of 7q32 in HB11 tumor was indicated. Because of the hypermethylation at the maternally methylated *MEST*-DMR, the paternal allele would have been lost. (C) Higher maternal copy number of 19q13 were suggested in HB11 tumor, based on the allelic ratio of *D19S589* and the hypermethylation at the maternally methylated *PEG3*-DMR. (D) Allelic copies of 20q11-q13 in HB05 and HB11 tumors were suggested to be abnormal by the allelic ratios of *D20S438* and *D20S158*. Based on the abnormal methylations at the paternally methylated *NESP*-DMR, HB05 tumor would carry more maternal copies than paternal copies of the locus, whereas in HB11 tumor, the paternal allelic copy number would be higher. (PDF 584 kb)

Abbreviations

DMR: Differentially methylated region; LOH: Loss of heterozygosity; UPD: Uniparental disomy; LINE-1: Long interspersed nuclear element-1; ICR: Imprinting control regions; BWS: Beckwith-Wiedemann syndrome; MALDI-TOF MS: Matrix-assisted laser desorption/ionization time-of-flight mass spectrometry; SNP: Single nucleotide polymorphism; COBRA: Combined bisulfite restriction analysis.

Competing interests

The authors declare that they have no competing interests.

Authors' contributions

JMR made significant contributions to the acquisition and analysis of data and also helped in manuscript preparation. TM, KH[1], HY, and KN[1] made contributions to technical supports and data analyses. RS, KM, RH, KK, YO, TS, TT[3], and TT[8] prepared the tissue samples. KN[5] and KH[5] performed technical support and statistical analyses. SA performed HE analyses of tumor samples. HS conceived the study, participated in its design and supervision and prepared the manuscript. KJ also participated in the design and supervision of the study and the preparation of the manuscript. All authors read and approved the final manuscript.

Acknowledgements

We thank Prof. Yutaka Kondo, Division of Epigenomics, Aichi Cancer Center Research Institute, Japan for technical advices in LINE-1 methylation analysis. This study was supported, in part, by a Grant for Research on Intractable Diseases from the Ministry of Health, Labor, and Welfare; a Grant for Child Health and Development from the National Center for Child Health and Development; and, a Grant-in-Aid for Challenging Exploratory Research and a Grant-in-Aid for Young Scientists (B) from the Japan Society for the Promotion of Science.

Author details

[1]Department of Biomolecular Sciences, Division of Molecular Genetics & Epigenetics, Faculty of Medicine, Saga University, Nabeshima 5-1-1, Saga 849-8501, Japan. [2]Faculty of Medicine, Sam Ratulangi University, Manado, Indonesia. [3]Department of Pediatric Surgery, Faculty of Medicine, Kyushu University, Fukuoka, Japan. [4]Department of Pediatrics, Toho University, Omori Medical Center, Tokyo, Japan. [5]Department of Maternal-Fetal Biology, National Research Institute for Child Health and Development, Tokyo, Japan. [6]Department of Pathology and Microbiology, Division of Pathology, Faculty of Medicine, Saga University, Saga, Japan. [7]Department of Anatomic Pathology, Pathological Sciences, Graduate School of Medical Sciences, Kyushu University, Fukuoka, Japan. [8]Department of Pediatric Surgery, Graduate School of Medical Science, Kyoto Prefectural University of Medicine, Kyoto, Japan.

Received: 13 March 2013 Accepted: 20 December 2013
Published: 27 December 2013

References

1. Herzog CE, Andrassy RJ, Eftekhari F: **Childhood cancers: hepatoblastoma.** *Oncologist* 2000, **5**(6):445–453.
2. Tomlinson GE, Kappler R: **Genetics and epigenetics of hepatoblastoma.** *Pediatr Blood Cancer* 2012, **59**(5):785–792.
3. Tomizawa S, Sasaki H: **Genomic imprinting and its relevance to congenital disease, infertility, molar pregnancy and induced pluripotent stem cell.** *J Hum Genet* 2012, **57**(2):84–91.
4. Murrell A: **Genomic imprinting and cancer: from primordial germ cells to somatic cells.** *ScientificWorldJournal* 2006, **6**:1888–1910.
5. Choufani S, Shuman C, Weksberg R: **Beckwith-Wiedemann syndrome.** *Am J Med Genet C: Semin Med Genet* 2010, **154C**(3):343–354.
6. Scelfo RA, Schwienbacher C, Veronese A, Gramantieri L, Bolondi L, Querzoli P, Nenci I, Calin GA, Angioni A, Barbanti-Brodano G, *et al*: **Loss of methylation at chromosome 11p15.5 is common in human adult tumors.** *Oncogene* 2002, **21**(16):2564–2572.
7. Honda S, Arai Y, Haruta M, Sasaki F, Ohira M, Yamaoka H, Horie H, Nakagawara A, Hiyama E, Todo S, *et al*: **Loss of imprinting of IGF2 correlates with hypermethylation of the H19 differentially methylated region in hepatoblastoma.** *Br J Cancer* 2008, **99**(11):1891–1899.
8. Chitragar S, Iyer VK, Agarwala S, Gupta SD, Sharma A, Wari MN: **Loss of heterozygosity on chromosome 11p15.5 and relapse in hepatoblastomas.** *Eur J Pediatr Surg* 2011, **21**(1):50–53.
9. Holm TM, Jackson-Grusby L, Brambrink T, Yamada Y, Rideout WM, Jaenisch R: **Global loss of imprinting leads to widespread tumorigenesis in adult mice.** *Cancer Cell* 2005, **8**(4):275–285.
10. Ehrich M, Nelson MR, Stanssens P, Zabeau M, Liloglou T, Xinarianos G, Cantor CR, Field JK, van den Boom D: **Quantitative high-throughput analysis of DNA methylation patterns by base-specific cleavage and mass spectrometry.** *Proc Natl Acad Sci U S A* 2005, **102**(44):15785–15790.
11. Woodfine K, Huddleston JE, Murrell A: **Quantitative analysis of DNA methylation at all human imprinted regions reveals preservation of epigenetic stability in adult somatic tissue.** *Epigenetics Chromatin* 2011, **4**(1):1.
12. Bollati V, Baccarelli A, Hou L, Bonzini M, Fustinoni S, Cavallo D, Byun HM, Jiang J, Marinelli B, Pesatori AC, *et al*: **Changes in DNA methylation patterns in subjects exposed to low-dose benzene.** *Cancer Res* 2007, **67**(3):876–880.
13. Roebuck DJ, Aronson D, Clapuyt P, Czauderna P, dJe Ville de Goyet J, Gauthier F, Mackinlay G, Maibach R, McHugh K, Olsen OE, *et al*: **2005 PRETEXT: a revised staging system for primary malignant liver tumours of childhood developed by the SIOPEL group.** *Pediatr Radiol* 2007, **37**(2):123–132. quiz 249–150.
14. Higashimoto K, Nakabayashi K, Yatsuki H, Yoshinaga H, Jozaki K, Okada J, Watanabe Y, Aoki A, Shiozaki A, Saito S, *et al*: **Aberrant methylation of H19-DMR acquired after implantation was dissimilar in soma versus placenta of patients with Beckwith-Wiedemann syndrome.** *Am J Med Genet A* 2012, **158A**(7):1670–1675.
15. Tost J, Dunker J, Gut IG: **Analysis and quantification of multiple methylation variable positions in CpG islands by Pyrosequencing.** *Biotechniques* 2003, **35**(1):152–156.